

Review

# Modelling of Spouted and Spout-Fluid Beds: Key for Their Successful Scale Up

Cristina Moliner <sup>1,\*</sup> , Filippo Marchelli <sup>2</sup>, Barbara Bosio <sup>1</sup> and Elisabetta Arato <sup>1</sup> 

<sup>1</sup> Dipartimento di Ingegneria Civile, Chimica e Ambientale (DICCA), Università degli Studi di Genova, Via Opera Pia 15, 16145 Genova, Italy; barbara.bosio@unige.it (B.B.); elisabetta.arato@unige.it (E.A.)

<sup>2</sup> Faculty of Sciences and Technology, Libera Università di Bolzano, Piazza Università 5, 39100 Bolzano, Italy; filippo.marchelli@natec.unibz.it

\* Correspondence: cristina.moliner@edu.unige.it; Tel.: +39-010-353-2588

Received: 30 September 2017; Accepted: 24 October 2017; Published: 28 October 2017

**Abstract:** The development of robust mathematical models could provide the necessary tools for a more rapid, efficient, and reliable spouted bed technology development. Computer simulations can be very useful to aid this design and scale-up process: firstly, they can contribute to obtain a fundamental insight into their complex dynamic behavior by understanding the elementary physical principles such as drag, friction, dissipation etc.; secondly, the simulations can be used as a design tool where the ultimate goal is to have a numerical model with predictive capabilities for gas-particle flows at engineering scale. Clearly, one single simulation method will not be able to achieve this goal, but a hierarchy of methods modelling phenomena on different length and time scales can achieve this. The most fruitful approach will be when they are simultaneously followed, so that they can mutually benefit from each other. In this sense, this paper presents a review of the current state of the art of modelling on spouted and spout-fluid beds through an analysis of recent literature following a multiscale approach (molecular and particle, lab, plant and industrial scale). The main features of the different scales together with their current limits are discussed and specific topics are highlighted as paths that still need to be explored. In summary, the paper aims to define the theoretical setline and the basis of improvement that would lead to a robust multiscale model with solid links between micro and macroscopic phenomena. If done with the correct balance between accuracy and computational costs it will gear SB towards their reliable and successful implementation.

**Keywords:** spouted and spout-fluid bed; modelling; multiscale approach; scale-up; CFD; multiphase flows

## 1. Framework of the Experimental Applications of the Technology

Spouted and Spout-Fluid Beds (SB) have been object of intense research during the past decades. The terms spouting and spouted bed were given by [1] at the National Research Council (NRC) of Canada to describe an innovative device based on fluidization technologies. Gishler and Mathur described this technology as “a flowing mechanism for solids and gas different from fluidisation but it achieves the same purpose for coarse particles as fluidisation does for fine materials”. In contrast with traditional fluidization [2], the fluid flow enters into the spouted bed through a single central inlet orifice creating three well differentiated zones: the central core of the reactor through which air flows is the spout, the surrounding annular region is the annulus and the solids above the bed surface entrained by the spout and going down the annulus form the so-called fountain. As an example, Figure 1 shows the different stages of spouting from the static bed situation (a) to a fully developed spouting regime (b) where the three previously mentioned zones can be easily identified.



**Figure 1.** Stages of spouting: from static bed (a) to a fully developed spouting regime (b).

Spout-fluid beds are a type of spouted bed in which, in addition to the central orifice, an auxiliary fluid flows through a series of holes in a surrounding distributor as shown in Figure 2 (white circles). This configuration makes a hybrid reactor that shares some characteristics of both spouting and fluidisation, which is especially useful for coarse, sticky or agglomerating solids.



**Figure 2.** Spout-fluid configuration.

Due to this particular configuration, the overall bed becomes a composite of a dilute phase central core and a dense phase annular region where a systematic cyclic pattern of solids movement is established giving rise to a unique system more suitable for certain applications than conventional fluidization techniques. Indeed, the existence of the described differentiated zones or the fact that usually coarse particles are present in the system leads to the need of finding different modelling approaches respect to those already existing for other types of fluid-solid configurations.

SBs were first applied as an alternative for the drying of badly slugged and moist wheat particles [1,3]. The vigorous movement of particles inside the reactor enabled the drying of the grain without damaging it. Soon, more applications were studied, and interest in these devices has been triggered in recent years being currently applied in a broad range of industrial applications, mostly related to drying processes, due to the high fluid-solid contact achieved.

Drying of barley malt [4], paddy rice [5] or mixtures of agricultural wastes [6] are the most traditional applications of SB as well as their use with pastes, slurries [7,8] and sludge from industry wastewaters [9]. In particular, SB have been widely applied in food industry for drying fruits and vegetables like red guava [10], acerola juice [11], cashew apple juice [12], peppermint [13], carrot cubes [14] or papaya seeds for oil production [15]. More recent developments have resulted

in the coupling of SB with additional techniques to increase the drying efficiency of the process. For example [16], studied a solar-assisted SB for the drying of pea while the application of microwave assisted technologies shows an increasing trend for a number of materials as fish [17], coffee beans [18], potato [19] and apple cubes [20], mushrooms [21] and green soybean [22].

SB devices are also extensively applied for coating of solids such as soybean seeds [23], nuclear fuel [22–26], group B iron powders [27], aerogels [28], urea [29] or polymethyl methacrylate [30]. Spouted beds are also used as chemical reactors to carry out, for example, benzyl alcohol polymerisation reactions [31], the production of hydrogen from the reforming of ethylene glycol with olivine [32], the synthesis of ceramic polymer composites [33–35], wastewater treatments [36–38] and electrochemical reactions [39,40].

Finally, thermo-chemical reactions are becoming an increasing field of application for SB reactors [41]. Pyrolysis of biomass [42–47], waste plastic [48,49], scrap tires [50,51] and sludge [52–55] have been tested and validated at lab and pilot scale. Also, the combustion of wood charcoal [56], biomass [57–59], sludge from the paper industry [60] or eventually toxic wastes [61] has been object of several studies as well as the gasification of coal [62,63], biomass [64–67], sewage sludge [68], flame retardants textile products [69] and mixtures of biomass with plastics [46] or coal [70].

However, even though the extensive research performed mainly at lab scale and, more recently, in fully developed pilot plants [63,67,68,71–73], there is still a lack of technical information regarding specific scaled-up solutions. To the knowledge of the authors, only one industrial-scale prototype has been developed for the continuous drying of paddy able to handle 3500 kg/h and temperatures up to 160 °C [74]. In this framework, modelling activities play a key role for the successful development of the technology. If well-developed, they are able to provide important information for the design and scale-up stage by describing in deep detail all the involved phenomena from a general and a more specific point of view.

For the specific case of SB, one of its main features should be to provide fundamental insights into its complex and particular fluid dynamic behaviour based on its characteristic elementary theoretical principles for drag, friction or dissipation phenomena. Moreover, modelling is a design tool whose ultimate goal is to obtain a numerical model with predictive capabilities in large scale applications. This description cannot be achieved with the application of a single method, but with the coupling of a hierarchy of methods able to describe different time and length scales. The most fruitful method will be that in which all the scales are solved simultaneously so they all benefit from each other.

In this sense, and for the purpose of this review, four different scales have been analysed and discussed according to the traditionally distinguished scales [75]. First of all, molecular and particle scale ( $10^{-9}$ – $10^{-1}$  m) is applied to study the kinetics, particle-fluid interactions (drag forces) and particle-particle interactions (collisions described by solid pressures and viscosities). The inclusion of the kinetic theory of granular flow permits the description of the system in a larger scale and the achievement of correlations to design SB devices (lab scale: 0.1–1 m). These correlations, together with the information of a precise framework and application, are used to define the operational parameters at plant scale (1–10 m). Even though high efforts have been performed in each of the mentioned scales, industrial scale (10 m) is still far beyond the capabilities of the current state of modelling.

More precisely, Figure 3 shows a scheme of the methodology of analysis performed in this work and the involved levels of study that will be studied in detail in the following sections.

Interactions between phases (fluid-solid, solid-solid, solid-walls) together with chemical reactions and their kinetics represent the core of the technology. Optimised mass and heat transfer rates are the result of the high contact between phases and, in this sense, the study of parameters like distribution of phases and their velocity profiles become essential to understand in great detail the involved phenomena. However, this area is to be explored with large number of incognita still to be resolved. In order to evaluate the current status, Section 2 presents a state of the art of modelling at molecular and particle scale and the coupling of mass and energy transfer phenomena with kinetic reactions.

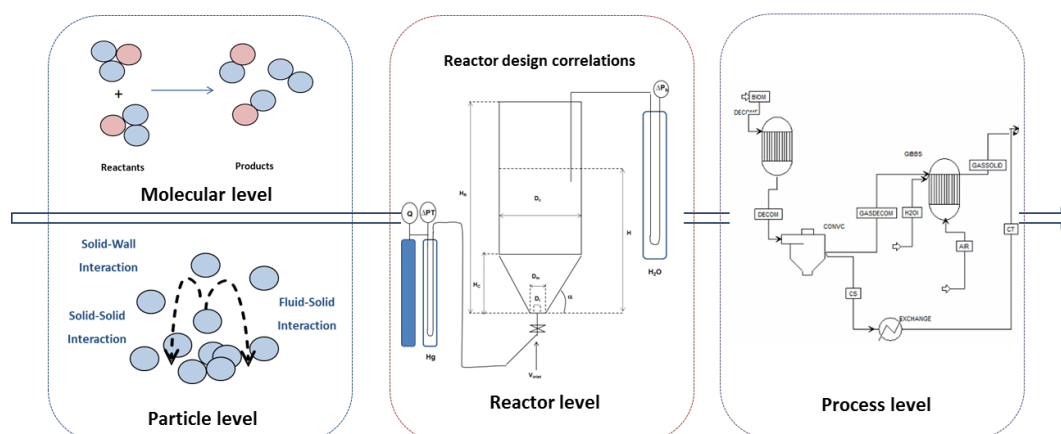


Figure 3. Multiscale analysis strategy.

In a successive level of detail, the description of the reactor (size, characteristic parameters, presence of auxiliary devices) plays a decisive role in its scale-up. The obtaining of correlations that permit to calculate the main design parameters (minimum spouting velocity or maximum pressure drops) in a larger scale is crucial. In this framework, Section 3 provides the main theoretical and operational mathematical descriptions of the reactor and a review of the most adequate developed correlations which are, however, highly dependent on the type of reactor or feedstock used for its obtaining.

The study of process applications in terms of applied operational conditions and their optimization to maximise efficiencies while minimising resources and costs is dealt in Section 4 with an insight to the main process software used in chemical engineering.

Finally, Section 5 presents an incipient modelling methodology based on the application of neural networks for the prediction of the main SB parameters in a non-mechanistic. Although in its early stages, the increase of experimental data could boost their application in a wider framework.

Verification is of high importance in modelling activities. In this sense, all the examined works refer to models that have been validated with experimental data either from activities carried out by the same authors or with data already available in literature.

In summary, SB seem a promising technology with few pilot plants already working but still lack of consolidated industrial applications. The definition of a robust and reliable model capable to be transferred to novel environments with successful results will be in high part the key of a successful commercial establishment (Figure 4).

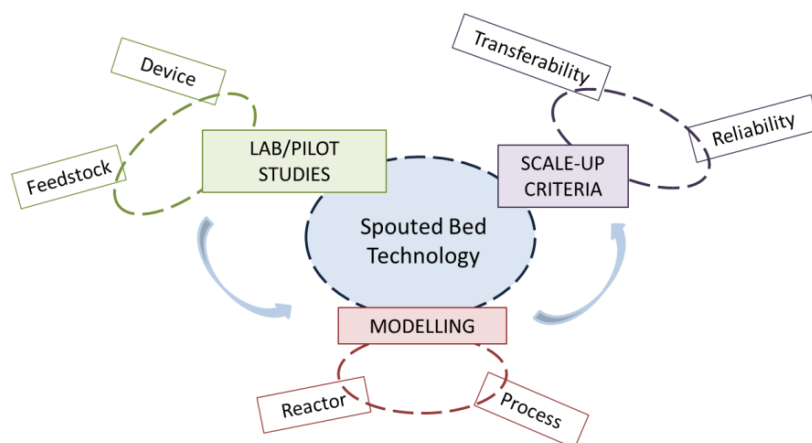


Figure 4. Levels of development of SB technology.

Within this framework, the main objectives of this work are:

- To set the current baseline of modelling in SB through the application of a multiscale analysis methodology, focusing the attention on the most recent works available in literature;
- To identify the critical aspects and remaining uncertainties where efforts still need to be done to achieve a better comprehension of phenomena;
- To suggest potential paths to be explored to foster the development of the technology.

In summary, the paper aims to contribute in the definition of the role of modelling for the complete establishment of the SB technology towards their reliable and successful implementation.

## 2. Molecular and Particle Scale Modelling

Kinetic rates and mechanisms at molecular level and the complex phenomena taking place at particle scale must be thoroughly understood when developing new processes. Especially when chemical reactions are involved, it is important to know how molecules behave and react in order to obtain the desired products, and how solid particles move and mix within the reactor volume. The ultimate goal will be to couple kinetic models with methods able to resolve the local balances of mass, momentum and energy in an efficient way. That way, the whole set of phenomena that take place within the device may be considered simultaneously, reproducing them with great accuracy and detail. As explained in the following sections, examples of this coupling are scarce.

### 2.1. Kinetic Modelling

Kinetic models provide essential information to quantify the conversion degrees and rates of specific reactions and to define the involved reaction mechanisms. As described in Section 1, a wide range of applications can be found for SB reactors and thus, a wide variety of related kinetic expressions are available in literature. However, only few works deal with the insertion of these expressions into more complex models which take into account the actual design and operational conditions of the reactor. It is clear that extensive experimental activities are required in order to achieve reliable kinetic laws. Also, the fact that kinetic models contain very specific parameters related to a specific process limits their applicability. In any case, the lack of implemented solutions using the already available expressions evidences a black hole in research on SB reactors.

One of the few works dealing with the implementation of kinetic rates on SB modelling was done by Kechagiopoulos et al. [76]. In it, the methane steam reforming was studied and its kinetic rates were added to the mass and energy balances. The model differentiated the spout and the annulus taking into account their different fluid dynamic properties and balances at each separate zone. As closure equations, interchange of mass and energy through the spout-annulus interface were considered. The model was further used to assess the influence of different factors (inlet velocity, temperature, bed height) on the efficiency of the process and the results proved that SB were good performing reactors for highly endothermic reactions.

A multiscale model to describe the yeast drying in a conical spouted bed was developed by Spreutels et al. [77] where the drying kinetics of a single pellet were combined with a gas–solid flow model with good agreement with the experimental results.

One of the main applications for SB nowadays is their use as reactors to carry out thermo-chemical reactions. Extensive research has been performed in order to obtain the kinetic parameters which better define the conversion reactions for biomass [78–81], biochar [82], plastics [48,80,83] or waste tires [84]. More precisely, the kinetic law required for large scale autothermal operation for the development of a conical SB reactor to obtain bio-oil was addressed by [85]. The study confirmed that, although the conditions of work applied in thermogravimetric analysis (TGA) are very different from those in real scale applications (heating rate, gas residence time, biomass particle size), the results from the kinetic models showed good agreement with the experimental values validating this approach as suitable for large scale conditions.

A SB reactor was used to experimentally calculate the kinetic rate of the pyrolysis of polyethylene terephthalate (PET) in the temperature range of 450–560 °C at two particle sizes (0.1–1.0 mm and 1.0–3.0 mm) in order to study potential heat and mass transfer limitations [83]. The similarity between the kinetic results revealed that heat and mass transfer limitations had been minimized. The results were compared with those obtained by isothermal Thermogravimetric Analysis (TGA) confirming the validity of the calculated kinetic expressions. A conical SB reactor was also used to obtain the kinetic expressions defining the catalytic cracking of the volatiles compounds formed in the flash pyrolysis of high density polyethylene (HDPE) on a catalyst based on HZSM-5 zeolite [86]. The catalyst deactivation was also considered inside the expression and was found to be dependent on the product concentration in the reaction medium. The model presented good agreement with experimental results and enabled the possibility to minimise the catalyst deactivation step.

In any case, the application of the calculated kinetic laws using lab-scale facilities for industrial scale applications, even though the mentioned successful applications, is still quite controversial, as several of the most important parameters could get very different values when the reactor is scaled-up (i.e., residence time, composition and dimensions of feed, ...). A correct assessment of the diffusional and heat transfer limitations will be required in each specific case to ensure a correct kinetic definition of the system for any feedstock and condition of work. In addition, a lack of kinetic equations representing the reactions involving the production of tar and high hydrocarbon compounds in SB reactors is evident and represents a path that needs to be explored.

## 2.2. Modelling Based on the Eulerian-Lagrangian Approach

The two most applied approaches for the simulations of granular materials are the Discrete Element Method (DEM) and the Two Fluid Model (TFM), also known as Eulerian-Lagrangian and Eulerian-Eulerian approach respectively. The former considers both the solid and the gas phase as interpenetrating continua and is feasible for industrial-scale facilities, but is highly dependent on parameters. The second tracks the trajectory of each discrete particle, thus representing the most natural choice at this scale, but is more computationally complex and can be used up to lab-scale devices within an acceptable calculation time.

The DEM approach was first proposed by Cundall and Strack [87]. The solid phase is constituted by discrete particles, each of them being tracked separately solving the Newtonian equations of motion. Due to its nature, it allows the obtainment of a significant amount of insights regarding the local behaviour of particles. Moreover, being more realistic from a physical point of view, it requires a limited amount of closure equations [88] (usually those accounting for the drag and the collisions). Works in which the same experiments are simulated through different approaches [89–92] show that the Eulerian-Lagrangian approach is the most accurate in reproducing the motion of particles.

The Lagrangian approach permits to avoid relying on a model accounting for the behaviour of granular materials; the development of a model satisfyingly describing the motion and mechanisms of granular materials is still an open challenge: it was indeed included in the 125 big questions [91] in a special issue celebrating the 125th year of publication of Science (“Can we develop a general theory of the dynamics of turbulent flows and the motion of granular materials?”). Its main drawback, however, is the substantial computational complexity it entails. Even with the achievements of modern computers, this approach is still only applied on a scale of 0.1–1 m, i.e., not at industrial scale [93]. Industrial-scale facilities usually contain up to trillions of solid particles, whereas DEM simulations usually consider about  $10^5$  particles; the largest DEM simulation analysed by the authors for this review evaluated the behaviour of 4.5 million particles, it employed 16 CPU and still required months of computational time [94]. However, Golshan et al. reported that for systems with a low number of particles, the Lagrangian approach may require less computational time than the Eulerian approach [91].

Recently, DEM has been employed for the simulation of SB by several researchers, as can be seen in Table 1. In general terms, all the reviewed works of this paper refer to simulations validated with experimental data and have been carried out at room temperature, unless stated otherwise.

**Table 1.** Works on CFD-DEM modelling of SB.

Geometry	Number of Occurrences	References
Spouted	17	[91,95–110]
Spout-Fluid	21	[89,90,92,111–128]
Other	10	[129–138]

Previous literature works summarising the state of art on CFD modelling of SB [139,140] highlighted the lack of a deep comprehension of the physical behaviour of the solid phase and the absence of a common agreement between researchers on the most accurate models and parameters for several simulated physical features, emphasising the role of turbulence. This feature, as shown in the following paragraphs, is still open in more recent works.

Regarding the employed software, Table 2 summarises the selected choices (where stated) to perform DEM calculations; from the existing multiple options it can be assumed that none of them is more used respect to others and the choice is up to the demand of each case. As an example, a DEM simulation of a binary mixture of glass beads using ANSYS FLUENT 17.0 is reported in Figure 5.

**Table 2.** Software used for DEM modelling in SB.

Program	Number of Occurrences	References
FLUENT	7	[89,106,111,117,134,136,141]
MFIX	6	[96,98,99,105,135,137]
OpenFOAM	4	[97,112,120,130]
EDEM	4	[100,101,133,138]
FORTRAN code	4	[119,125,130,142]
BARRACUDA	3	[89,90,131]
Self-made code	3	[107,108,118]
DEMEST	2	[90,92]
LIGGGHTS	2	[91,129]
GenIDLEST	1	[124]
XPS	1	[128]

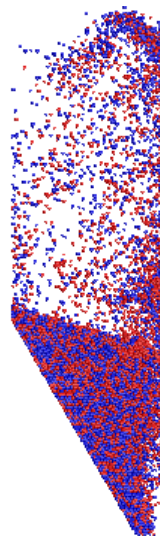


**Figure 5.** Spouting of a binary mixture of glass particles in ANSYS FLUENT 17.0.

In order to achieve convergence, the cells of the computational grid must be bigger than the simulated particles. As a consequence, especially for coarse particles (common in spouted beds), the computational grid cannot be very fine, possibly compromising the accuracy of the calculation for the fluid phase. In particular, Liu and colleagues [88] suggested that the diameter of the computational cell should be set to 5–10 times the diameter of the biggest particle, while Li and co-workers [112] showed that a ratio between the grid size and the particles diameter inferior to 1.67 generated problems in the calculation of particles motion. Alobaid [90] proposed that the ratio between the dimensions of cell and diameter should be between 2 and 3; indeed, this offset method was employed for the simulation of a lab-scale spouted-fluid bed, confirming its accuracy [126]. In another work [122], the employment of two different grids for the fluid and solid phase with different sizes was proposed to improve the accuracy of the calculation.

Performing calculations in irregular geometries can be challenging when a coarse mesh is used; in fact, spout-fluid beds have no inclined walls and that permits the use of a more regular mesh. In this sense, spout-fluid beds are more abundant in DEM simulations compared with those performed with TFM, as it can be seen in Table 1 and Section 3.2. A group of researchers from the Zhejiang University employed a geometry with a zig zag wall instead of an inclined one in two different works [103,104] to reproduce the experiments performed in a spouted bed with a conical base by Vieira Neto et al. [143].

A common feature of all DEM works regards the calculation of collisions between particles, where three approaches exist: the soft-spheres approach, the hard-spheres approach and the statistical approach. The soft-spheres approach [87] is the most widespread, with almost all works on DEM modelling of spouted beds employing it (including all of the works reported in the following sections unless stated otherwise). It considers that particles deform when colliding, but instead of actually deforming them (which would require additional equations), it lets them slightly overlap and calculates the effect of the collision as a function of the overlapping. The main forces influencing the trajectories of particles are gravity ( $F_g$ ), drag ( $F_D$ ) and the collision forces ( $F_c$ ); they are schematised in Figure 6.

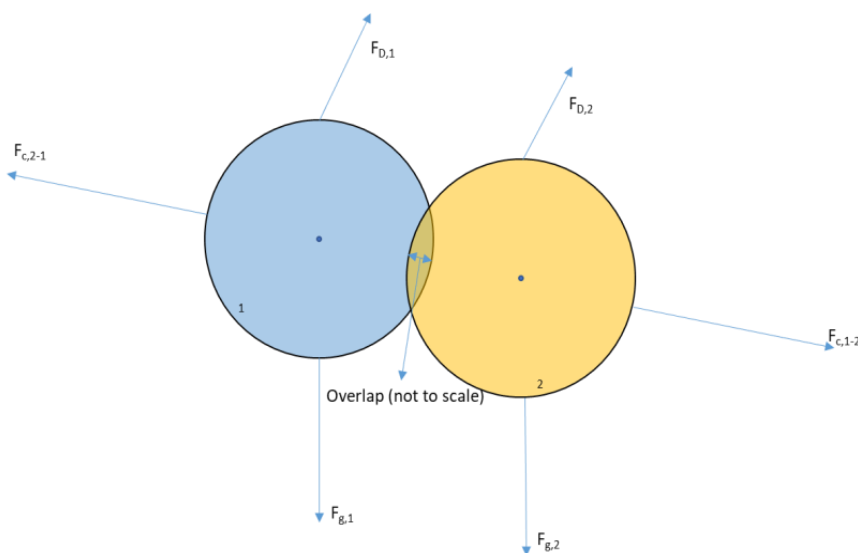


**Figure 6.** Main forces acting on two colliding particles in the soft sphere approach.

There are several mathematical approaches [144] with the so-called spring-dashpot model commonly used which considers a spring and a dashpot accounting for the repulsive force and the collision inelasticity, respectively. A number of parameters must be specified for the spring-dashpot model; most notably, the spring constant has a relevant role: the higher it is, the smaller the time step must be [88] extending the computational time of the simulation. The value of the constant depends on the material and is hard to measure experimentally. Di Renzo and Di Maio [145] developed a complex

non-linear model to predict the value of the constant yielding values between  $10^5$  and  $10^8$  N/m; however, previous works by Tsuji and others [146,147] showed that increasing the value over certain orders of magnitude has little effect on the accuracy of the simulation, and suggested setting it to 800 N/m. Other works proved that, for non-cohesive particles, simulations are insensitive to the value of the spring constant [148,149], and thus setting it to a low value does not hinder the simulation accuracy. In most works, the value of the constant is reported to be between  $10^2$  and  $10^6$  N/m.

The two other approaches are less common. The hard-spheres approach considers collisions as quasi-instantaneous, binary and punctual [150]. The statistical approach, instead, considers specific particle properties in a continuum framework, and collisions are thus calculated in a statistic way [151]. Hoomans [152] found out that, if the spring stiffness is high enough, the hard and soft spheres models produce very similar results.

The hypotheses behind DEM and its models (as the drag law), take into account both the behavior of a single particle, and the influence of the surrounding ones. Indeed, this leads to different effects, such as the different velocities and volume fraction of particles in the three characteristic zones of SBs (spout, annulus and fountain). In the reported works, comments on these features were sometimes addressed, usually pointing out the different behaviour of the particles and the exchanges between two adjacent zones. In other rare cases, the authors reported observations on the formation of bubbles or on the movement of clusters of particles. Nonetheless, more effort should be put on this direction, given the potential of DEM for the assessment of the local behaviour of solids; for example, no work addressed phenomena such as the rotation of clouds of particles or the effect of the particles volume fraction on the velocity of the gas phase.

Finally, another possible feature of particles can be cohesiveness (for wet/sticky particles). However, all discussed works consider non-cohesive particles, if not stated otherwise. DEM simulation of granular systems still has a number of open questions [153] as it will be discussed in the following sub-sections. Nonetheless, the development of more complete models has permitted the study of several features of SB achieving an initial and successful insight on the fluid dynamic characteristics of the technology.

### 2.2.1. Optimisation of Drag Laws

Several drag correlations which account for the interaction between the fluid and the solid phase have been developed throughout the years. However, there is still no consensus regarding which one can reproduce more accurately every feature of the motion of particles in spouted beds and its choice is not explained by the authors in most DEM works. The selected models in the works considered for this review (where stated) are reported in Table 3.

**Table 3.** Drag models used in DEM simulations.

Drag Law	Number of Occurrences	References
Gidaspow [154]	18	[91,96,97,103,104,111,113,116–120,124,125,130,138,141,155]
Koch and Hill [156]	7	[90,95,99,105,129,135,137]
Beetstra [157]	3	[121,127,129]
Syamlal-O'Brien [158]	3	[89,134,136]
Wen-Yu [159]	3	[90,109,131]
Hill et al. [160]	2	[92,115]
Dahl and Hrenya [161]	1	[98]
Di Felice [162]	1	[101]
Haider and Levenspiel [163]	1	[106]
Pepiot and Desjardins [164]	1	[128]
Ren et al. [165]	1	[102]
Van der Hoef et al. [166]	1	[112]

Although the Gidaspow drag model represented the most common choice, other models were often selected and indeed some works focused their attention on the comparison of drag laws to define the most suitable one.

More recently, Pietsch et al. [129] reported that Koch and Hill's [156] and Beetstra's [157] drag laws, based on Lattice-Boltzmann simulations, were the most adequate to reproduce the motion of particles in their prismatic spouted bed. Zhang and Li [98] argued that the drag coefficient is a 2nd order tensor, which can be reduced to a homogeneous function. They implemented several drag models and defined the one by Dahl and Hrenya [161] as the most accurate for a spouted bed.

Li and co-workers [112] assessed the most adequate drag law for a spout-fluid bed. The van der Hoef [166] and Gidaspow [154] laws produced the best results regarding the bubble formation whereas the van der Hoef and Beetstra were the most adequate for the spout-fluidisation regime. However, none of the studied relationship was free of flaws.

The validity of three drag laws (Gidaspow, Syamal-O'Brien and Wen-Yu) was tested in a spout-fluid bed by Zhou and others [111]: they reported that all three laws could accurately reproduce the spouting evolution of the bed, but the bed height was always underestimated. They identified Gidaspow law as the most accurate drag model, although pointing out that much work still has to be done in this field.

The Beetstra drag model was employed for the simulation of a spout-fluid bed with draft plates by Sutkar et al. [121]. They obtained a satisfactory agreement thanks to the hypothesis that the annulus motion might be better reproduced with the inclusion of a rolling friction model.

From the above considerations, it is clear that an agreement on the most suitable drag model is definitely lacking in DEM simulations. Similarly to the main drag law, additional drag models can simulate the effect of secondary physical phenomena; the most common ones are the Saffman force and the Magnus lift effect which are taken into account in some works [90,116,118,141,167], and neglected in others [101,106,112,120,129].

### 2.2.2. Definition of Particles

When specifying the properties of particles, two problems arise, one related to the number of particles, and the other to their shape. Researchers may try to diminish the number of particles in order to reduce the computational complexity. One of the most common approach consists in employing the so-called parcels instead of actual particles; they are computational particles which have different diameters than those of the actual particles whose behaviour are reproducing. Drag and other effects are calculated according to the theoretical diameter, but collisions according to the diameter of the parcel. Big parcels may however require a coarse mesh, lowering the accuracy of the simulation.

Lu and colleagues [168] employed simulations of a bubbling fluidised bed to show that when parcels account for several real particles, the mesh size is significantly coarse and some sub-grid features of the motion of the solids might be not reproduced, unless structure dependent sub-grid drag models are used, such as the energy-minimisation multi-scale (EMMS)/bubbling drag model [169]: these are different from (semi-)empirical drag models and Direct Numerical Simulations-based correlations, which are homogeneous, because they take into account the effect of heterogeneous structure, such as bubbles and clusters.

Four different scaling approaches and a full scale approach were tested in the simulation of a spout-fluid bed by Banerjee and Agarwal [114]: one based on parcels, one proposed by Glicksman et al. [170], one proposed by Link et al. [171], and one based on the terminal particle velocity, proposed by the authors. Banerjee and Agarwal [114] found that their method was both the most reliable in reproducing the behaviour of particles and the most efficient in reducing the number of simulated particles, thus optimising the computational time. Some of the aforementioned scaling approaches were also tested through DEM simulations in spout-fluid beds by other researchers: Sutkar et al. [127] reported the validity and efficacy of the Link et al. one in significantly reducing the

computational time, and Ebrahimi and colleagues [128] verified the suitability of the Glicksman et al., both in a pseudo-2D and a 3D case, which also led to speed up the simulation.

Another commonly employed approach to reduce the total number of particles consists in decreasing the depth of the bed. This was done by Qiu and co-workers [99] who compared a slot-rectangular spouted bed simulating it both in 3D and quasi-3D. The results were similar although a few differences could be pointed out: increasing the depth, the pressure drop and minimum spouting velocity decreased at first and then reached an asymptotic value; bubbling internal jet regime and steady spouting regime could not be observed in the quasi-3D model; the maximum spring height and spout diameter were higher in the 3D simulation. In another study, Marchelli et al. [106] observed that the onset spouting velocity of homogeneous and binary mixtures of particles could be well predicted by means of a pseudo 2D geometry employing parcels which are bigger or smaller than the actual particles.

In several processes, particles are not perfect spheres and defining their exact shape is of key importance for the accuracy of the calculation. Nonetheless, developing and solving laws for non-spherical particles is extremely complex and, even though some examples exist in literature, not all CFD programs offer the possibility of simulating them [172]. In an attempt to account for different shapes, the Haider and Levenspiel drag law [163] takes into account the increased surface area of non-spherical particles (when compared to spherical particles of equal volume) increasing the drag coefficient of particles.

A typical compromise between complexity and physical plausibility is the application of the ‘multi-sphere method’, where non spherical particles are defined as two or more intersecting spheres. The first reported study in which the multi-sphere method was applied for a spouted bed is by Ren and colleagues [107], who simulated corn-shaped particles constituted by four or seven spherical elements, highlighting that the first choice allowed better reproduction of experimental data (minimum spouting velocity and fountain height). The developed methodology was employed [108] for the study of mixing of binary mixtures of corn-shaped and spherical particles (see Section 2.2.5). The same group [102] also applied this method to simulate cylindroid particles by comparing the results produced by an own-developed drag law [165] able to predict the fluid dynamics and pressure drop of non-spherical particles with those obtained with the Wen-Yu drag law. Also, when compared to spherical particles, cylindrical particles produced a more irregular fountain, especially for high values of the static bed height.

When considering a realistic system, it cannot be neglected that particles may feature a wide size and shape distribution. In reacting systems, particles can shrink as reactions proceed. This may create a problem as taking into account small particles results in an increase of the total number of particles. Also, the lower the diameter of the smallest particle is, the lower the time step of the simulations must be set (when using a linear spring-dashpot collision model, the collision time is roughly proportional to  $d_p^{3/2}$ , with  $d_p$  being the diameter of particles). Both of these options result in an increase of the computational time and one should always choose a compromise between the physical plausibility and the feasibility of the simulation.

In a 2014 article, Berger and Hrenya stated that “DEM is far from being able to simulate realistically wide size distributions” [173], suggesting the use of continuum models for granular materials (such as the Eulerian-Eulerian one) for the scope. In fact, although the literature reviewed for this work was broad, no research dealing with multi-dispersed particulate systems in spouted beds was found which evidences a lack in PSD theoretical studies for SB.

### 2.2.3. Turbulence Modelling

The role of turbulence was not extensively discussed in most works regarding the CFD modelling of SB. Navier-Stokes equations were in most cases solved in their Reynolds-averaged form (RANS, Reynolds Averaged Navier Stokes), with the  $k-\epsilon$  model being the most common choice to calculate the turbulent viscosity; however, in many cases turbulence was entirely neglected. In addition, common

turbulence models consider additional differential equations that must be solved, increasing the complexity of the calculations. Approaches which rely on less simplifying hypotheses, such as the Large Eddy Simulations (LES), are even more demanding. In this sense, clarifying the necessity of turbulence modelling in spouted beds is of great relevance. A summary of the approaches to turbulence in the considered articles is presented in Table 4.

Some researchers [114] commented on neglecting turbulence stating that its effect is negligible when the volume fraction of the solid phase exceeds 0.001 [174]. Others [175], instead, run simulations to prove that the turbulence kinetic energy is very high in the interface zone between the spout and the annulus, and not employing a turbulence model hinders the accuracy of the results.

**Table 4.** Turbulence models used for DEM modelling in SB.

Model	Number of Occurrences	References
$k-\varepsilon$	22	[90,92,95,96,98,99,101,103–108,110,111,116,118,122,126,129,134,135]
None or not specified	18	[89,91,97,100,102,112–115,120,124,125,128,130–132,136,138]
Sub-grid Scale (SSG)	3	[117,121,127]
Large Eddy Simulation (LES)	2	[109,123]
RNG $k-\varepsilon$	1	[133]

Yang et al. [135] concluded that the influence of the turbulence model in a double slot spouted column was significant in the spout and fountain regions. Wang et al. [119] compared gas-solid heat transfer in a spout fluid bed, comparing the effects of including a turbulence model (not specified) or neglecting it; they showed that the inclusion of the model leads to more accurate results, but the difference is negligible, highlighting that the Stokes number of particle is low and thus turbulent diffusion does not affect heat transfer significantly. Saidi et al. [120] simulated a spout-fluid bed, neglecting the turbulence effects and obtaining good similarities with experimental data, including pressure drops. They observed that column thickness had an effect on the vertical flux of particles, hence confirming that the wall effect has a significant influence in thin beds.

A drawback of common turbulence models is that they contain empirical parameters (six for the  $k-\varepsilon$  model) and there is no consensus on their optimal value. For this reason, some researchers [109,123] employed the Large Eddy Simulation (LES) approach, which contains less parameters; in particular, Wang et al. [123] highlighted the better accuracy of the LES approach, commenting on the intensity of turbulence in various zones of a pseudo-2D spout-fluid column.

In another rare exception, Sutkar and colleagues [127] simulated turbulence in a spout-fluid bed employing a sub-grid scale (SGS) model proposed by Vreman [176], which entails less simplifying hypotheses.

#### 2.2.4. Study of the Fluidisation Behaviour

Predicting the fluidisation behaviour of solids is usually the main goal when modelling a spouted bed. To assess the validity of the simulation, results were usually compared with experimental voidage, velocity or pressure profiles.

The spouting behaviour of high-density particles (like those employed in nuclear operations) was studied by Li and colleagues [101] employing a pseudo 2D geometry, assessing the dependency of many variables on particle density. Most notably, they observed that minimum spouting velocity and peak pressure drop were proportional to  $\rho_p^{0.67}$  and  $\rho_p^{1.2}$  (with  $\rho_p$  being the density of particles) and that dense particles had a wider range of stable spouting state and a dual dominant frequency. Marchelli et al. [106] studied the effect of diameter, density and sphericity of particles on the onset spouting velocity in a pseudo 2D model, observing that the reliability of the predictions was comparable to the results obtained with the Mathur-Ghisler equation. In another work, the spouting of 6 mm

particles in a spouted bed was simulated by Yang et al. [110]; they observed that the flux of solids was dramatically higher in the axial than in the radial direction and the spout diameter increased with the gas velocity and with bed elevation. Also, the spout and annulus exchanged mass through all the interface, with the exchange being more intense with an increase of the gas velocity.

Rong and Zhan [141] employed a user defined function to insert DEM in an early version of FLUENT and validated their model with experimental analyses. Saidi and Tabrizi used DEM to prove that the use of an additional background gas flow in a spout-fluid bed eliminates dead zones [177]. Yang and collaborators [115] assessed the influence of several parameters on the solid dispersion in a spout-fluid bed, reporting that the increasing on the spouting and fluidisation velocities promoted it in the spout and fountain region in vertical and lateral directions, but had no effects on the annulus. Similar results could be obtained decreasing the particle size and the bed height or increasing the bed depth and the total gas flow rate.

The spouting behaviour of cohesive particles must be modelled with adequate hypotheses. Several models to calculate cohesive forces among particles can be found in literature. Different causes of cohesiveness can be taken into account, but they are complex and entail several parameters, hence not being very practical in their application. For this reason, Xu et al. [116] proposed a much simpler model, where cohesive forces were calculated multiplying a parameter (which varied from 0 to 20) by the gravitational force acting on each particle. When spouting developed, a cohesive force of ten times the gravitational force (roughly the force acting on wet particles) caused significant agglomeration of particles and when it was further doubled, the spout collapsed. The cohesive force reduced the velocity of particles, their concentration in the fountain and their recirculation flux. Zhang and Li [96] proposed a more detailed approach, which took into account both capillary and viscous forces, and applied it to monodispersed particles in a spouted bed. They validated it by comparison with several features observed in experiments, such as the fact that the frequency, velocity and fountain height were higher for wet rather than for dry particles. Moreover, they employed the resources of CFD to show that the granular temperature of wet particles was higher than that of the dry ones in the spout and fountain zones, while it is unchanged in the annulus.

#### 2.2.5. Particle Mixing

Spouted beds feature excellent mixing properties. When compared to standard fluidised beds [178], segregation phenomena in heterogeneous mixtures are significantly hindered, provided that the adequate operating conditions are selected [3,179]. Nevertheless, the mixing of particles differing in diameter, density and shape must be carefully evaluated prior to undergoing a desired process. In this framework, a validated CFD model is a powerful tool to assess the quality of solids mixing in spouted beds, offering detailed insights about zones where segregation might arise, especially if DEM is used to simulate the interactions between particles.

Wen and colleagues [100] evaluated different mixing indexes. Among them, the neighbour distance method was considered the most suitable one, even though it should be modified in order to account for particles with different diameter.

Mixing might change whether particles are wet or dry, and Zhu et al. [142] studied the influence of both conditions using a monodispersed mixture of particles in a spouted bed. The Mikami model [180] was applied for wet solids and, as a result, an increase in the spouting velocity accelerated the mixing process whereas an increase in particle moisture decreased the velocity of particles, velocity gradient and mixing rate.

Mixing is influenced by the difference in physical properties of particles. Ren and co-workers [167] studied the effect of the density ratio in a spouted bed, finding out that the more this ratio was increased, the worse and more time demanding the mixing became. Similar features could be seen if the trajectories of two tracers were followed. However, the light tracer travelled to averagely higher positions in the fountain and had average longer cycle times, spending more time in the annulus,

probably because it landed at higher radial distance from the centre. The same effect was observed by Marchelli et al. [106] for a binary mixture of glass particles of different diameters.

In the only study of mixing of non-spherical particles in a spouted bed, Ren and co-workers [108] employed the multi-sphere method (see Section 2.2.2) to assess the behaviour of corn-shaped and spherical particles. They observed that monodispersed mixtures of spherical particles feature a faster mixing, while in equi-volumetric binary mixtures the quality of mixing is affected by the difference in properties, with size influencing it more significantly than shape; differences in shape, size and density concur in diversifying the trajectories of particles in the fountain region, hence hindering the mixing.

Karimi and Dehkordi [118] analysed the influence of diameter and density of binary mixtures in a spout-fluid bed. They confirmed that segregation was more severe when the difference of diameter and/or density of the two kinds of particles was greater and, in that case, a more intense gas flow rate is needed to achieve a good mixing state; in spout-fluid beds, axial segregation only occurred over a certain value of the bed height, while radial segregation had a more significant influence due to the presence of dead zones next to the gas inlet. In any case, the bed never reached a fully segregated state.

#### 2.2.6. Heat Transfer and Chemical Reactions

As described in Section 1, spouted beds are employed for coating and drying particles, and also as chemical reactors, mainly for catalytic, polymerisation and thermochemical processes. The inclusion of such physical and chemical phenomena in a CFD model is possible but complex, and increases the time needed to perform simulations.

Even though its importance, few works can be found in literature as reported by Zhong et al. [181] in a recent review on CFD simulation of Dense Particulate Reaction Systems (DPRS). The authors grouped the existing barriers for the wide use of DEM for DPRS in three points: the unsuitability of the current computational capacity for the simulation of industrial facilities, which would take years of simulation time to reproduce 30 s of a reactor's behavior; the current limitations in simulating non-spherical particles, fragmentation of particles and the evolution of their physical properties, such as density, porosity and composition and the lack of a more comprehensive model, which would permit to consider relevant secondary phenomena, such as the production of tar, char and pollutants or the erosion of the wall.

The correct inclusion of the energy balance equations is of key importance in the study of thermochemical processes. Wang et al. [119] modelled the cooling of particles, initially at 150 °C, when spouted by air flow at ambient temperature. The increase in the rate of the fed gas promoted the convective gas-solid and conductive solid-solid heat transfer in the jet, but hindered them in the annulus region; the temperature of particles was lower in upper sections of the bed, while that of the gas phase behaved oppositely.

In order to develop a preliminary model of coal-direct chemical-looping combustion with ANSYS FLUENT, Banerjee and Agarwal [132] successfully simulated a spouted bed reactor in which gaseous methane reacted with solid Fe-based oxygen carriers. The model had previously [136] been validated by comparison with cold-flow experiments, and the features of CFD modelling were exploited to improve the design of the reactor, enhancing the solid recirculation and avoiding dead zones. In the latter work, they pointed out that the output of the process strongly depended on the fluidisation quality: dense Fe<sub>2</sub>O<sub>3</sub> particles did not allow the obtainment of a good fluidisation regime, which was instead achieved with 60% Fe<sub>2</sub>O<sub>3</sub> supported on MgAl<sub>2</sub>O<sub>4</sub>. It is interesting to highlight that their model required 24 h of calculation time to simulate 200 ms of the reactor, showing the high time-consuming demand of these simulations.

Xie and collaborators [109] developed a complete 3D CFD-DEM model of a spouted bed gasifier, modelling turbulence with the Large Eddy Simulation (LES) model to successfully simulate the gasification of woody biomass. The results showed that high temperatures lead to instability in the gas-solid fluid dynamic regime and that part of the solids are oxidised in the higher part of the reactor, increasing the volume fractions of hydrogen and carbon dioxide.

### 2.2.7. DEM Applied to Auxiliary Devices

Several configurations or auxiliary devices can be included in SB to improve their spouting behaviour. The most commonly applied geometries are shown in Figure 7: conical (a), cylindrical (b) or prismatic (c) with the arrow indicating the inflow gas. The injection of gas can also be performed according to different base configurations as the traditional orifice of circular cross section (Figure 7d) or through a rectangular slot (Figure 7e).

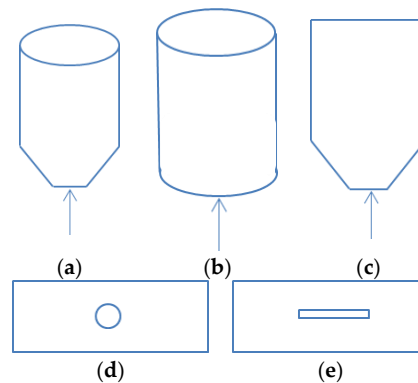


**Figure 7.** Different geometries applied in SB: conical (a); cylindrical (b) or prismatic (c); Injection of gas through circular cross section (d) or rectangular slot (e).

In addition, several auxiliary devices are used to improve spouting phenomena. Most notably, a draft tube which encloses the spout region can be added in order to make the flow more stable and gain a better control of the particle circulation pattern. Figure 8 shows a scheme with the most applied devices: porous/non-porous draft tubes (a), porous/non-porous draft plates (b) or the recently proposed fountain confiners (c) specifically used to improve the stabilization of the process with fine particles.

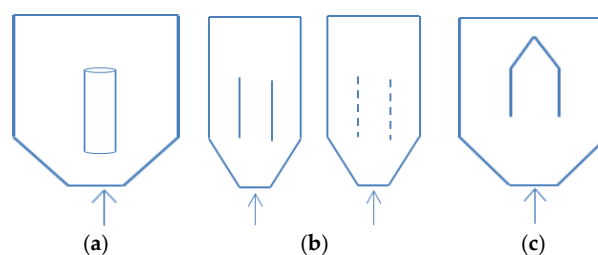


**Figure 8.** Scheme of possible auxiliary devices used with SB: porous/non-porous draft tubes (a); porous/non-porous draft plates (b) or the recently proposed fountain confiners (c).

An analysis with Fast Fourier Transform (FFT) allowed Pietsch and co-workers [129] to observe that the spouting behaviour (initially instable) of a 3D prismatic spouted bed with two horizontal gas inlets could be enhanced by the addition of two draft plates. This is mostly promising for processes with liquid injections. Similarly, Salikov et al. [133] modelled a prismatic spout-fluid bed with two horizontal gas inlets obtaining similar flow features. Fries and colleagues [138] compared three different granulators, one of them a prismatic spouted bed, and evaluated their fluid dynamics and collision intensity in order to predict the properties of the produced particles.

The circulation of solids within a spouted bed with and without a draft tube was investigated by Luo and colleagues [104] who highlighted the substantial differences observed: the solids dispersion took place in different zones, being more intense when the draft tube is used. They also showed that the extension of the draft tube over the bed surface makes the solid circulation more vigorous.

A model of a slot-rectangular spouted bed was developed and validated by Saidi et al. [97]. They observed that the particle fluxes were higher when the bed height was increased and that, in higher horizontal sections of the bed, the spout shape became less rectangular and more circular.

The effect of the angle of the inclined wall of a slot-rectangular spouted bed was studied by Golshan and others [95], who employed a pseudo 2D open-source model previously developed by Zhao et al. [175]. They assessed how the angle affected the minimum spouting velocity, proposing a new correlation for its calculation. They also observed that an increase of the angle (i.e., making the device wider) enhanced the velocity of particles and solid flux in the central zone and proposed a novel curved bed which displays improved particles circulation performance.

Wang et al. [130] simulated a dual-column slot-rectangular spouted bed featuring a suspended partition, which kept the two fountains separated; they obtained good similarity with their experimental results, pointing out that the initial position of the suspended partition had little influence on the stable spouting conditions and that increasing the gap below the partition enhanced the solids transfer between the two columns. The simulations considered about 97,000 to 140,000 particles and, in order to reproduce 20 s, up to 2 months of calculation time were needed. Yang et al. [135,137] studied a double-slot spouted column too, employing 112 CPUs to simulate the behaviour of more than 2.5 million particles; the model had already been validated for a single slot spouted bed [105], by comparison of the pressure drop and velocity profiles. For the double-slot device they observed that, thanks to the partition plate, there is little exchange of information between the two partitions, which display good symmetry properties. In addition, doubling the chambers causes an increase in the pressure drop and minimum spouting velocity.

Deb and Tafti [124] modelled a spout-fluid bed to investigate the effect of employing one, two or three separate gas inlets; they reported that pressure drop is lower when only one inlet is used, and examined several methods to assess the mixing quality as a function of the number of jets used and the superficial gas velocity.

Adding draft plates to a spout-fluid bed increased the symmetry of the spouting channel, reduced the instability of the pressure drop and decreased the gas leakage from the spout to the annulus as explained by Yang and collaborators [113]. However, if the plates were too long, solid recirculation rate was reduced concluding that the optimal length must be a trade-off between the positive and negative effects. Sutkar et al. [127] studied a spout-fluid bed with draft plates, with the aim of validating a scaling approach; the bed was considered composed either of glass or of  $\gamma$ -alumina particles, and a good matching with experimental data was obtained in the reproduction of the motion of particles within the device.

Draft tubes might get damaged during operation when subjected to severe operating conditions or collisions with solids. In order to account for this effect, Yang and colleagues [103] included the Finnie erosion model [182] in their simulation of a spouted bed with a draft tube: they observed that, regardless the tube configuration, erosion is more pronounced in the upper region of the tube. They also proved that the increase of the tube height over the bed surface enhanced erosion whilst the reduction of the entrainment distance minimised it. Regarding the fluid dynamics, they observed that the insertion of a draft tube regularized the movement of particles inside the reactor. Moreover, there was less leakage of gas in the annulus and the solid vertical flux was promoted by increasing the length of the tube above the bed surface or increasing the entrainment zone.

Zhang and colleagues [131] reproduced a spouted bed employed as a pneumatic transporter of oil shale semi-coke particles. The model was validated by comparisons of the pressure drops, velocity and volume fraction distributions, and the feasibility of the process was proved.

### 3. Lab Scale Modelling

Spouted beds can be more practically modelled through a methodology established on a lab scale. This methodology may be mainly based on correlations or CFD models based on the Two Fluid Model (TFM) approach.

In general, correlations are easy to use and, in many cases, very reliable. However, the complexity of the fluid dynamics of SB has hindered the development of robust correlations for SB based on theoretical considerations; indeed, most of them are developed in order to fit the highest number of experimental data. Also, the TFM approach, compared to the DEM approach, provides less details on a particle scale, but it is a more practical tool to model lab scale (or larger) devices due to its lower computational cost. As its main drawback, its sensitivity to physical parameters is highly significant.

### 3.1. Modelling Based on Semi-Empirical Correlations and Dimensional Similitude

Due to the complex fluid dynamic nature of SB, their design and performance are still not completely well-understood. Indeed, a key factor for their successful scale-up is the correct assessment and control of the main operational parameters.

The minimum spouting velocity ( $U_{ms}$ ) is probably the most important parameter for SB. In terms of industrial design, the operational characteristics of the air blower according to the gas inlet requirements are one of the main factors that need to be evaluated as they are closely related to the reliability of the system, as well as to the costs of operation. In practical terms,  $U_{ms}$  is defined as the minimum gas inflow required for maintaining stable spouting conditions and it is closely dependent on the geometrical characteristics of the reactor and the physical properties of the solid phase. For this reason, extensive research is dedicated to obtain a reliable equation for a wide range of operational conditions. However, most of them have been only validated for a specific range of study and fail to predict most of the design variables when conditions are changed, especially for large devices which tend to be less stable and therefore, harder to control and operate.

Due to the large range of parameters affecting the spouting process, a great number of correlations for  $U_{ms}$  have been developed according to the specific characteristics of the device and process.  $U_{ms}$  for conical, cylindrical and flat reactors is well represented (about  $\pm 10\%$ ) by the Mathur-Ghisler equation [1], applied for ambient conditions and diameter of reactor ( $D$ ) lower than 0.5 m. As stated before, almost all equations proposed in literature apply to  $D < 0.5$  m. One of the few equations proposed for larger diameters is the equation by Fane and Mitchell [183] which, in essence, is an empirical modification of Mathur and Ghisler equation based on measurements on a device with  $D = 1.07$  m, highlighting the lack of information regarding  $U_{ms}$  in large units. Moreover, few correlations [50,184] have been developed with a varying temperature, which in practice varies the density and viscosity of the inflow gas. A summary of the most applied equations is presented in Table 5.

**Table 5.** Most applied correlations for  $U_{ms}$ .

Authors	Correlation
Mathur and Gishler (1955) [1]	$U_{ms} = \left(\frac{d_p}{D}\right) \left(\frac{D_i}{D}\right)^{\frac{1}{3}} \sqrt{\frac{2gH(\rho_p - \rho)}{\rho}}$
Fane and Mitchell (1984) [169]	$U_{ms} = 2D^{1-\exp(-7D^2)} \left(\frac{d_p}{D}\right) \left(\frac{D_i}{D}\right)^{\frac{1}{3}} \sqrt{\frac{2gH(\rho_p - \rho)}{\rho}}$ for $D > 0.4$ m
Olazar et al. (1994) [185]	$U_{ms} = \left(\frac{d_p}{D}\right) \left(\frac{D_i}{D}\right)^{0.1} \sqrt{\frac{2gH(\rho_p - \rho)}{\rho}}$
Li et al. (1996) [184]	$U_{ms} = 1.63U_t \left(\frac{d_p}{D}\right)^{0.414} \left(\frac{D_i}{D}\right)^{0.127} \left(\frac{H_m}{D}\right)^{0.452} \left(\frac{\rho_p - \rho}{\rho}\right)^{-0.149}$ based on high temperature data
Anabtawi et al. (1992) [186]	$U_{ms} = 2.44 \left(\frac{d_p}{D}\right)^{0.7} \left(\frac{D_0}{D}\right)^{0.58} \left(\frac{H}{D}\right)^{0.5} \left[\frac{2gH(\rho_p - \rho)}{\rho}\right]^{0.28}$ for square column

The applicability of the equation of Mathur-Gishler for mixtures was also evaluated and the expression was found valid if the average particle diameter and average particle density is calculated by  $d_p = 1 / \sum \left( \frac{x_i}{d_{pi}} \right)$  and  $\rho_p = 1 / \sum \left( \frac{x_i}{\rho_{pi}} \right)$ , respectively, with  $x_i$  being the mass fraction of species  $i$ .

More recently, an experimental campaign using five types of biomass and a device with non-porous and open-sided draft tubes was carried out by Saldarriaga et al. [187] to obtain correlations valid for the calculation of  $U_{ms}$  using particles of low density and different sphericity values.

Other important parameters to be defined in the design of SB are the maximum and stable pressure drops. The pressure drop of a system is closely related to its energy requirements. Its correct assessment is crucial to optimise the operational conditions and the associated costs. As a rough approximation, the maximum pressure drop is 1.5–2.5 times higher than the stable value. Once again, the currently available correlations lack of a wide framework of valid conditions where they can be successfully applied and so, their use is restricted to the range of parameters from which they were obtained. Table 6 gathers the most widely applied equations for the calculation of the maximum ( $\Delta P_M$ ) and stable ( $\Delta P_S$ ) pressure drops.

Although relatively often neglected over other fluid dynamic parameters, the fountain area in SB is an important design input. It defines the required total height of the device and the freeboard area above the static bed. Furthermore, the fountain is even more important in SB reactors as reactions might be occurring in that region and, depending on the fountain temperature or amount of solids/gas present, unselective reactive pathways might become activated, consuming/producing preferential products.

**Table 6.** Most applied correlations for  $\Delta P_M$  and  $\Delta P_S$ .

Authors	Correlation	Geometry
Manurung (1964) [188]	$\frac{-\Delta P_M}{\rho_b g H} = \left[ 0.8 + \frac{6.8}{\tan \gamma} \left( \frac{D_i}{D} \right) \right] - \frac{34.4 d_p}{H}$	Cylindrical
Olazar et al. (1994) [185]	$\frac{-\Delta P_M}{\Delta P_S} = 1 + 0.35 \left( \frac{H}{D_i} \right)^{0.1} \left( \frac{D_i}{D} \right)^{1.1} Ar^{0.1}$	Cylindrical
Kmiec (1980) [189]	$\frac{-\Delta P_M}{\rho_b g H} = 1 + 0.206 \exp \left( \frac{1.24 H}{D} \right)$	Conical
Olazar et al. (1993) [190]	$\frac{-\Delta P_M}{\Delta P_S} = 1 + 0.116 \left( \frac{H}{D_i} \right)^{0.5} \tan \left( \frac{\theta}{2} \right)^{-0.8} Ar^{0.0125}$	Conical
Markowski and Kaminski (1983) [191]	$\frac{-\Delta P_S}{\rho U_{ms}^2} = 0.19 \left( \frac{D}{H_0} \right)^{0.56} \left( \frac{D_i}{H_0} \right)^{2.39} \left( \frac{H_0}{d_p} \right)^{2.35}$	Conical
Olazar et al. (1993) [190]	$\frac{-\Delta P_S}{H_0 \rho_p (1 - \epsilon_0) g} = 1.20 \left( \tan \left( \frac{\gamma}{2} \right) \right)^{-0.11} (Re_{ms})^{-0.06} \left( \frac{H_0}{D_i} \right)^{0.08}$	Conical

Fountain height increases with increasing air inflow and decreases with increasing particle size and shape factor and the diameter of the spout is usually much higher than the inlet diameter. As an example, one of the few correlations for their calculation are the following [192]:

$$H_f = 1.01 \times 10^{-2} \gamma^{-0.14} \left( \frac{D_0}{D_i} \right)^{1.14} \left( \frac{D_i}{d_p} \right)^{0.83} \left( \frac{H_0}{D_0} \right)^{-0.52} \left( \frac{U}{U_{ms}} \right)^{4.8} \rho_p^{-0.12} \phi^{-1.45}$$

$$D_s = 0.52 G^{0.16} D_i^{0.41} \gamma^{-0.19} D_b^{0.8} \left( \frac{U_i}{U_{ms}} \right)^{0.8}$$

Averaged cycle times and fountain heights were successfully predicted by the one-dimensional model by Olazar et al. [193] using  $U_{ms}$  and the pressure drop evolution as inputs. These parameters are of great importance in the definition of operational times (especially for batch experiments) and for the geometric factors of the reactor. Moreover, the simplicity of the model permits the coupling of fluid dynamic properties with kinetic ones for a more complete reactor design. Even though this model successfully predicted the solid and gas velocity profiles, it failed to describe the particle velocity along the spout. This weakness was overcome by Niksiar et al. [194] through the application of a

streamtube modelling approach which permitted the obtainment of a more accurate prediction of the radial distribution of gas and particle velocities inside the SB.

Finally, the maximum bed height ( $H_m$ ) is defined as the highest bed able to be spouted and represents the limit of material which can be processed by a SB. McNab and Bridgewater [195] proved valid the following equation:

$$H_m = \frac{D^2}{d_p} \left( \frac{D}{D_i} \right)^{\frac{2}{3}} \frac{568b^2}{Ar} \left( \sqrt{1 + 35.9 \times 10^{-6} Ar} - 1 \right)^2$$

with  $b = 1.11$ , which gave the best fitting to experimental data in gas spouted-beds at room temperature. At different operational conditions,  $H_m$  decreases with increasing temperature and with decreasing pressure.

At larger scale, only the equation of Lefroy and Davidson [196] is an alternative to estimate  $H_m$  in columns with  $D > 0.5$  m.

$$H_m = 0.68D^{4/3}/d_p^{1/3}$$

Another strategy for scale-up activities is to use a set of dimensionless groups to be matched to maintain the fluid dynamic similarity between reactors. This dimensional similitude methodology is widely employed in different fluid dynamic applications as aircraft and ship design, and has become popular in scaling of fluidized beds. With this purpose He et al. [197] proposed the following dimensionless parameters (extrapolated from fluidised reactors) for a bed of fixed geometry:

$$\frac{g \cdot d_p}{U^2}, \frac{\rho_p \cdot d_p \cdot U}{\mu}, \frac{\rho}{\rho_p}, \frac{H}{d_p}, \frac{D}{d_p}, \phi, \gamma, \varepsilon_0$$

where  $g \cdot d_p / U^2$  is the Froude number,  $\rho_p \cdot d_p \cdot U / \mu$  is the Reynolds number,  $\rho / \rho_p$  is the ratio of fluid density to particle density,  $H / d_p$  is the ratio of bed height to particle diameter,  $D / d_p$  is the ratio of column diameter to particle diameter,  $\phi$  is the sphericity of particles,  $\gamma$  is the inertial friction angle of particle and  $\varepsilon_0$  is the loose packed voidage.

These groups are the same as those proposed by Glicksman [198] with the addition of  $\varepsilon_0$  and  $\phi$  to take into account the more frequent particle–particle interactions and the greater compression and friction forces in SB relative to conventional fluidized beds.

Following this approach, studies have been conducted to expand the dimensionless-groups of spouted beds by adding the restitution coefficient ( $e_s$ , which accounts for the inelasticity of particles collision) or the friction of particles [199]. This parameter becomes crucial due to the important role that the interparticle collisions play in the fountain and spout regions.

As an evaluation of this approach, the scale-up methodology was carried out using sophisticated optical fibre probes that measured simultaneously the local velocity of solids, normal and shear stresses and turbulent kinetic energy [200]. The study evidenced the need of local measurements of hydrodynamic parameters for the correct scale up procedures. In addition, a recent work by Aradhya et al. suggested that current dimensionless groups are not sufficient to explain the complete hydrodynamics of the spouted bed system [201]. A new mechanistic methodology of scale-up for gas-solid spouted beds was proposed considering the similarity in local hydrodynamics based on maintaining similar radial profiles of gas holdup in the scaled-up units.

This approach however is only suitable for ‘cold’ scale-up (i.e., modelling of hydrodynamics) and it can only be extrapolated to other physical phenomena such as heat transfer if it is possible to match other key dimensionless groups. However, it is unlikely to be suitable for situations with more complex phenomena as substantial temperature or concentration gradients or chemical reactions.

### 3.2. Modelling Based on the Eulerian-Eulerian Approach

Spouted beds can be efficiently simulated at a lab-scale through CFD models employing the so-called Eulerian-Eulerian approach or Two-Fluid Model (TFM). In this approach, both the fluid and

the solid phases are treated as mutually interpenetrating continua, and their behaviour is predicted through the numerical solution of mass, momentum and energy balance equations. Obviously, such a hypothesis for the solid phase is most appropriate if the particles composing it are very small, so that their macroscopic behaviour can be roughly compared to that of a continuum. The balances must be coupled in order to predict the momentum exchange between the two phases, and further equations must be specified to describe turbulence, interfacial forces, solid stress and other factors.

The advantage of this approach is its relatively low computational complexity, which allows its employment even on a physical scale of 1–10 m, i.e., at plant level. The drawbacks are the loss of information regarding the local behaviour of particles and the significant amount and influence of parameters and closure equations required for an accurate reproduction of the experimental findings. The works considered in this review are summarised in Table 7. As discussed in Section 2, all the presented models have been validated with experimental data obtained at room temperature, unless stated otherwise.

**Table 7.** Works on CFD-TFM modelling of SB.

Geometry	Number of Occurrences	References
Spouted	28	[25,91,202–227]
Spout-Fluid	7	[89,90,92,228–231]
Other	1	[232]

Overall, as already stated in Section 2.2, TFM has been employed less than DEM for spout-fluid beds but still appears to be the first choice for spouted beds.

The Kinetic Theory of Granular Flow (KTGF) has been used in all simulations of spouted bed reactors employing an Eulerian approach, with no exceptions; details about its theoretical development can be found in the work of Gidaspow [233]. In short, it relies on the definition of solid ‘pressure’, ‘viscosity’ and the ‘granular temperature’. KTGF can recreate the behaviour of spouted beds with great accuracy provided each parameter is properly specified. However, Sun et al. [117] employed DEM to simulate a spout-fluidised bed and evaluated the translational, rotational and configurational temperature of particle. The results showed that KTGF was incapable of accurately predict solid pressure, shear viscosity, granular conductivity and kinetic energy dissipation when the volume fraction of particles was high.

Contrarily to DEM simulations, all of the works discussed in the following paragraphs employ (where stated) the commercial CFD program ANSYS FLUENT; an example of a work performed with FLUENT and the TFM approach is shown in Figure 9. There is only one work employing ANSYS CFX, different from all the others as it regards the simulation of a SB containing water [217].

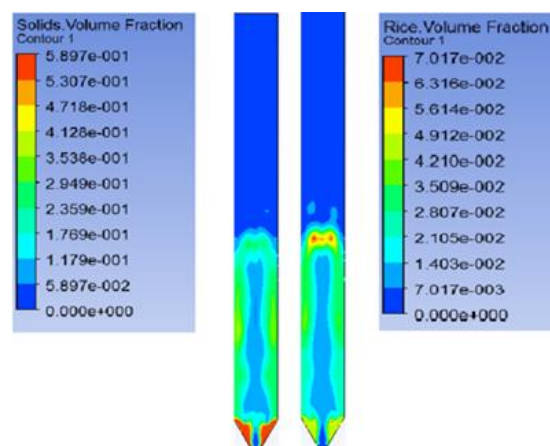


**Figure 9.** Volume fraction of sand (left) and rice straw (right) in a spouted bed.

### 3.2.1. Optimisation of Drag Laws and Coefficients

Drag models and coefficients cannot be experimentally measured but affect critically the behaviour of the solid phase. Similarly to DEM, a universally accepted set has not been identified yet, and an optimisation must be performed for each scenario. Table 8 summarises the selected drag models for the works presented in this review (where stated).

There are much less options than in DEM and it is evident that the Gidaspow and Syamlal-O'Brien drag models were the preferred choices, with other models being rare exceptions.

As in DEM works, extensive research was devoted to the identification of the most suitable model for drag and other coefficients. Moreover, given the complexity of the KTGF, identifying the most suitable values for the parameters involved was mandatory in order to successfully perform simulations.

Hosseini and co-workers [227] employed the KTGF to model a cylindrical spouted bed and analysed the influence of a great number of simulation variables. Drag and solid shear viscosity had the most relevant influence and the use of the representative unit cell (RUC) drag model and the Syamlal et al. viscosity model was suggested. Moreover, the use of an algebraic equation for the granular temperature was accurate enough if an adequate restitution coefficient was specified. They also pointed out that the higher the restitution coefficient was, the lower the fountain height tended to be.

For a spouted bed, Wang et al. [210] noted that the Huilin-Gidaspow drag coefficient under-predicted the bed pressure drop and fountain height, suggesting the implementation of a modified drag model to take into account more appropriately the effect of the wall on the flow.

The specular coefficient takes into account the friction between particles and the wall: it is an empirical parameter, whose limit values are 0 for perfect specular collisions and 1 for perfectly diffuse collision, depending on the roughness of the wall. Bettega and his colleagues [234] performed simulations in a pseudo-cylindrical (half-column) spouted bed, highlighting that the specular coefficient had a strong influence on the motion of the solid phase, but not on the static pressure, velocity of the particles in the bed and solid fraction in the spout. Fattahi et al. [228] emphasised the relevance of the specular coefficient too, identifying the most appropriate value for their case of study at 0.025 and encouraging the development of a correlation of this coefficient with different operational conditions.

Drag laws and specular coefficient were also studied by Setarehshenas and co-workers [205] for a conical spouted bed containing heavy zirconia particles with the aim of optimising the simulation procedure. Gidaspow was found the best fitting drag law and the use of a tetrahedral mesh could reduce the calculation time without ruining the accuracy. The specular coefficient significantly affected the behaviour of particles with an optimal value of 0.05. The particle-wall restitution coefficient did not influence the simulation: setting it as 1 or employing a no-slip boundary condition produced the same results.

The relevance of the specular coefficient also depends on the geometry: Hosseini and colleagues [220] modelled a pseudo 2D spouted bed both in a 2D and a 3D approach. They highlighted that the latter yielded more accurate results but was significantly more sensitive to changes to the particle-wall restitution coefficient and the specular coefficient (with best values found to be 0.2 and 0.05 respectively); nonetheless, they stressed out that the use of a complete 3D model was the best choice to accurately reproduce the bed behaviour.

**Table 8.** Drag laws used in TFM simulations.

Drag Law	Number of Occurrences	References
Gidaspow [154]	17	[25,91,204–206,208–210,213,218,220,222,226,228,229,234,235]
Syamlal-O'Brien [158]	14	[89,90,92,114,203,207,214,215,224,225,230–232,236]
RUC [237]	1	[227]
Esmaili and Mahinpey [238]	1	[221]

### 3.2.2. Turbulence Modelling

Turbulence was not extensively discussed in most works and when considered, the  $k$ - $\epsilon$  turbulence model [239] was mostly employed. As it can be seen in Table 9, almost half of the works did not include a turbulence model.

**Table 9.** Turbulence models.

Model	Number of Occurrences	References
$k$ - $\epsilon$	18	[90,92,203,204,206,209,211,212,215–218,223–227,230–232,236]
None or not specified	16	[25,89,91,202,203,205,207,208,210,213,214,220–222,228,229]
$k$ - $\omega$	1	[217]
Shear Stress Transport (SST)	1	[217]

Riera and co-workers [217] simulated a multi-phase spouted column to test the validity of three turbulence models: the  $k$ - $\epsilon$  model, the  $k$ - $\omega$  model [240] and the SST model [241]. They observed that the  $k$ - $\epsilon$  and  $k$ - $\omega$  models yielded similar results for an air-water mixture, while the SST model was the most adequate for the air-water-sand mixture.

For some researchers, the inclusion of turbulence complicates the model without significant benefits: Omar Reza et al. [203] argued in fact that the Reynolds number for particles inside the column can be estimated to be about 70. They performed simulations both in laminar conditions and with the  $k$ - $\epsilon$  dispersed turbulent model finding out that, in the bed region, the velocity and distribution of gas and particles were almost identical, but the behaviour of gas differed in the zone above the bed. In this case, Syamlal-O'Brien drag model best reproduced the experiments and a decrease in the value of the restitution coefficient made the volume-averaged velocities of gas and particles oscillate at a higher period.

### 3.2.3. Study of the Fluidisation Behaviour

Assessing the spouting behaviour of solids for different operating conditions is one of the main goals of CFD models, and it is especially useful for solids whose use is not completely established, such as irregular solids as corn [223].

After the validation of their model, using particles with diameter 1.44 mm, Tabatabaei and colleagues [221] employed it to obtain the complete regime map of a slot-rectangular spouted bed containing particles of diameter 3.77 mm; the momentum exchange between the solid and gas phases was calculated through a drag law they previously developed [238], which is a modification of the Di Felice [162] drag law. Jin and others [207,214] simulated the fluid dynamics of a spouted bed used as food Microwave Vacuum Dryer, obtaining that both the jet penetration depth and the pressure drop have an almost linear dependence on the spouting velocity.

Following an unusual CFD-based Equivalent Reactor Network (ERN) model, Du and colleagues [211] modelled the fluid dynamics of a spouted bed reactor employed as polyethylene gasifier to identify the separate fluid dynamics zone it features, and then considered each of them as a separate block in Aspen Plus<sup>®</sup> v7.3 (see Section 4).

Jin and co-workers [207] simulated the fluid dynamic behaviour of lettuce particles in a spouted bed in view of a microwave-vacuum drying application. The simulations confirmed that an increasing mass of lettuce required an increasing air flow rate to obtain the same flow pattern; moreover, it was observed that the penetration depth was proportional to the gas flow rate and that the pressure drop shifted from negative to positive values as the spouting velocity was increased. Şentürk Lüle et al. [25] proved that the TFM was able to reproduce a spouted bed operating with heavy zirconia particles (with density 6050 kg/m<sup>3</sup>), similarly to what happens in spouted nuclear fuel coat-ers.

### 3.2.4. Particle Mixing

Several groups employed the TFM approach to assess the mixing behaviour of binary or even ternary particles mixtures. As in the studies performed with the DEM approach, a common conclusion of most of these works was that, for each mixture, there was a value of gas velocity above which segregation was extremely mitigated or eliminated. This is not stated again in the following paragraphs, and only further findings are reported.

Usually, when segregation occurred, fine particles mainly circulated in the inner circle, and coarse particles in the outer, due to the difference in the gas-solid drag coefficient. This was observed by Du et al. [204] in a spouted bed; they showed that this effect was more visible for particles with different density rather than those with different diameter; all of their analysis were performed with particles with diameter of 0.39 mm as the first solid phase.

The behaviour of a binary mixture of particles with different density and diameter at various relative volume fractions was also studied by Wang and colleagues [230], who developed a 3D model of a two-jets spout-fluidised bed. Their work highlighted that segregation was mainly caused by the slight difference of velocity of the two solids around bubbles, while the circulating movement of particles caused by the two jets enhances the mixing. They concluded that segregation phenomena occurred more significantly for mixtures comprising equal volumetric amounts of the two solids, and that segregation was prevented when the two volumetric fractions were largely different. The difference in diameter was taken into account by Santos et al. [208], who reproduced the behaviour of a binary mixture of glass particles in a spouted bed. Larger particles were mostly present in the spout and in the middle of the annulus, with their concentration reaching a minimum between these two zones and near the wall.

Regarding more irregular solids, Bove and his collaborators [209] simulated the spouting behaviour of a mixture of silica and rice straw with the aim of gasifying the latter. They obtained good results in the reproduction of the fountain height but not highly accurate in the prediction of the pressure drop. Similarly, Melo and others [206] studied the behaviour of mixtures of sand and low density polyethylene (LDPE)/Al composites at several volumetric ratios for future pyrolysis applications. They employed the Gidaspow drag model and the dispersed  $k-\varepsilon$  turbulence model and good results were obtained, with errors in the pressure drop up to 35%.

A good mixing between solids is of key relevance for every process, but this is especially true when SB are used as plain mixers: Liu et al. [232] tested the effectiveness of an industrial-scale spout-fluid mixer of biomass and inert material with the aid of a CFD model. The mixer also had lateral gas inlets and could process 18.75 t/h of biomass in a continuous manner. A mixing effectiveness of more than 80% was achieved provided the optimal values for the spouting and the lateral gas flows were set. However, when the spouting velocity was increased, mixing was hindered because the trajectories of solids, fed from the upper part of the device, were affected; mixing also worsened if the lateral gas flow was higher than half of the spouting gas flow.

Eulerian-Eulerian simulations of solids with size distribution, as it can be the case of biomass, is more feasible than with the Eulerian-Lagrangian approach as the limitations related to the mesh size and time step do not apply. Nonetheless, no articles dealing with TFM simulation of such systems in spouted beds were found during the review period. Contributions to this interesting and useful research topic could represent a significant advance in the knowledge of spouted beds specially when applied to chemical processes.

### 3.2.5. Correlations, Dimensioning and Scale-Up Studies

TFM simulations can be effective tools to evaluate the validity of correlations and scale-up criteria. Scaled up columns were studied by Zhong et al. [225], assessing the effect of particle density and diameter, static bed height and gas inlet diameter on the  $U_{ms}$ . The model was previously validated with experiments and it was observed that the Mathur-Ghisler equation provides the most similar values of  $U_{ms}$  [224]. They pointed out that it increased as solid density and diameter increased, although less

intensely for larger columns.  $U_{ms}$  also increased when the static bed height was increased and the fluid inlet diameter was decreased, with a more remarked effect for larger columns. The approach was further applied [215] to a spouted bed operating under high pressure conditions (up to 10 MPa), as it could happen in industrial applications: it was seen that  $U_{ms}$  decreased with increasing pressure, whereas the associated gas mass flow rate increased. Having set the gas velocity to  $1.2 U_{ms}$ , an increase in the pressure established a higher and more stable fountain in a shorter time; pressure also affected the distribution and velocity of particles.

Spouted columns of different scales were studied by Du et al. [222]: among their findings, they saw that  $U_{ms}$  decreased as the column diameter was increased so they suggested paying attention to the ratio between the diameters of the inlet and of the column; moreover, given that all the scaling parameters were verified, it can be seen that in larger columns the dimensionless fountain height was higher and voidage profiles were different. Based on these observations, they proposed new scaling relations for the spout diameter and  $U_{ms}$ .

A scale-up relationship for spouted beds was proposed by He et al. [197]; Bettega and colleagues [235] verified its validity with a 2D model, confirming that when the scaling relationships were not satisfied, the hydrodynamics of the beds was severely hindered.

### 3.2.6. Heat Transfer and Chemical Reactions

The Eulerian-Eulerian approach allows taking into account heat transfer and chemical reactions, although problems can arise while doing so. In their 2016 review, Zhong and colleagues summarised the limitations of this approach for the simulation of Dense Particulate Reaction Systems (DPRS) [181]. Even if TFM is generally faster than DEM, considering chemical reaction increases the computational time by about 1.6 times, defining the limits for the simulation of industrial units, especially if their additional unit operations are considered. Moreover, the simplifying hypotheses of TFM could lead to inaccuracies when wide particles diameter distributions are modelled, as well as for the variation of the diameter of particles and inter-phase mass exchanges. In general, DPRSs seem to be more frequently simulated through the Eulerian-Eulerian approach [181], but this is not the case of spouted bed reactors.

Fattahi et al. [228] simulated a spout-fluidised bed fed with air with increasing temperature; the interphase heat transfer was modelled through an approach proposed by Gunn [242], which correlated the Nusselt and Reynolds numbers and the Prandtl number. In accordance with their experimental data, the temperature distribution was not uniform, with peaks in the central spout, slightly above the inlet, and in the fountain top. The same authors followed an analogous approach in a subsequent work [229] to test the influence of 5 radial distribution functions (which correct the collision probability for a dense medium) on the hydrodynamics and heat transfer. The distribution of solids was better predicted by the function of Lun and Savage, while the thermal comparison showed that Lun and Savage's [243] function could better predict the temperature of particles near the wall, while those by Ma and Ahmadi [244] and Arastoopour [245] yielded better results in the fountain region.

Fluidised beds may be designed with a conical inlet in order to promote a fluid dynamic regime similar to that of a spouted bed. Such a device was studied by [213] for CO<sub>2</sub> removal via adsorption, with a CFD study on the heat transfer between wall and bed; it was observed that 75 µm particles behaved like a spouted bed, while 375 µm behaved like a fluidised bed and, thanks to the simulations performed, the heat transfer coefficients were estimated.

### 3.2.7. TFM Applied to Auxiliary Devices

Liu and colleagues [236] assessed the influence of the conical base angle on the spouting regime; they found out that the spouting was unstable for angles inferior to 30°, and that the fountain height and spout diameter had a maximum angle of 105°. Also, the velocity of particles in the annulus kept increasing as the angle was further increased. The effect of the conical angle was also studied by the group of Setarehshenas [202] who employed a FLUENT model of a spouted bed previously

validated [205]. For heavy zirconia particles, the angle strongly affected the hydrodynamic regime and small angles led to incoherent spouting; they also showed that considering a half-column model with a wall in the symmetry plane did not reproduce the velocity profile of the spout of a full column. Only a study by Liu and colleagues [212] was devoted to evaluate the performances of alternative gas inlets in spouted beds: they studied traditional and modified single nozzle inlets, multiple nozzles inlet and swirl flow inlet, pointing out that only the latter can lead to a more uniform spouting, as a consequence of a reduction of the aggregation of particles near the wall and the increase of the gas-particles contact efficiency.

On the basis of simulations of a spouted bed with a draft tube, Hosseini and collaborators [218] showed that the influence of the specular coefficient and the particle–wall restitution coefficient was particularly relevant in the prediction of the velocity profiles inside the draft tube, suggesting respective optimal values of 0.05 and 0.2 (even though other combinations yielded acceptable results). In general, a study on the optimal value of this parameter should always be performed when simulating a new device, especially in spouted beds with draft tubes; moreover, the accuracy of the model depends significantly on the inclusion of the frictional stress. Moradi et al. [226] simulated a spouted bed with a draft tube too and showed that an increase in the height of the tube leads to instability in the motion of particles.

A way to increase the flux of gas is to allow the flow of gas also through a grid from the conical part; Wang and collaborators [216] simulated this in a spout-fluid bed. They observed that the fountain had a low height and the gas volume fraction was still minimum in the annulus, even though the annulus was dispersed, the solid volume fraction was the most uniform with the angle between the horizontal direction and the fluidising gas jets equal to  $45^\circ$ .

Spouted and spout-fluidised beds may be scaled-up by assembling multiple units (example shown in Figure 10). Chen et al. [246] simulated a multiple spout fluidised bed assessing the effect of baffles, which divide the bed in three parts. They showed the effect was different depending on the number of gas inlet used: positive in case of double and triple spouting and negative in case of single spouting; moreover, in case of multiple spouting, the fountains may disturb each other creating more difficulties in the development of a stable regime.

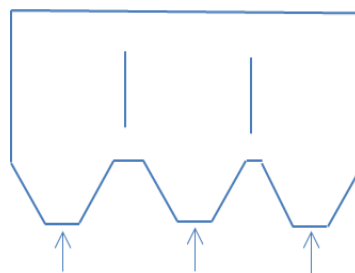


Figure 10. Example of assembly of multiple units.

#### 4. Plant Scale Modelling

Experimental trial and error tests provide the most reliable data to evaluate the behaviour of new units within a specific framework, even though they are expensive both in time and economic terms. There is, however, a major drawback: the change of one of the parameters of the process may lead to different optimum conditions. This is the case of size-dependent processes where the most adequate parameters found for the lab scale plant might be no longer valid for the scaled-up unit.

Modelling activities constitute a useful tool to evaluate industrial processes in a costless and non-time consuming way respect with experimental activities themselves. They can provide valuable information regarding the feasibility of a process using new feedstock or they can help predicting the behaviour of a system when the operational conditions are modified. Also, models may be used to

evaluate potential hazardous processes or to define the technological limits that a reaction can face due to either thermo-chemical or technical limitations.

In this context, commercial process simulators like Aspen Plus<sup>®</sup> v9, Comsol<sup>®</sup> v5.3, Chemcad<sup>®</sup> v.6.5 or Simulink<sup>®</sup> v.9.0 or the free-code COCO v.3.2 can be valuable tools to perform mass and energy balances in a low time consuming manner. It is obvious that, the more detailed the model is, the more accurate the predictions will be. It is thus necessary to define which are the main objectives of the model and evaluate its potential limitations due to the characteristics of the specific processes under study.

SB are increasingly being applied to perform thermo-chemical reactions. They can be modelled following an “equilibrium” approach considering that the process is fast enough and the time residence is long enough for the equilibrium state to be reached. Aspen Plus<sup>®</sup> v.8.0 was used to assess the feasibility of the gasification of rice straw and kaki residues in a SB reactor [247]. The equilibrium model is based on the minimisation of the Gibbs free energy and was aimed to predict the composition of the producer gas when different operational conditions (i.e., equivalence ratio, temperature, humidity) were varied. Jarungthammachote and Dutta [248] applied the non-stoichiometric equilibrium model to a central-jet, circular split spouted bed and spout-fluid bed. The initial model presented significant deviations from the experimental data, especially for CO and CO<sub>2</sub> due to the influence of the carbon conversion on the equilibrium assumption. The model was modified considering this effect and, as a result, its outcomes were much closer to the experimental data.

In addition to the definition of carbon conversion, the application of the “quasi-equilibrium temperature” (QET) approach is also considered a good strategy to correct potential deviations from an equilibrium situation. In QET, the equilibrium of reactions is evaluated at temperatures different than the actual process temperature. This approach has been applied by Moliner et al. [249] with the aid of Aspen Plus<sup>®</sup> (Temperature Approach option). The values of equilibrium temperatures were defined according to the results from Kersten et al. [250] and the results provided a more accurate feasibility analysis on the gasification of agricultural residues taking into account more realistic assumptions.

More sophisticated block abilities might be used to insert specific kinetics of reaction. Aspen Plus<sup>®</sup> can incorporate FORTRAN subroutines to account for expressions which are not provided as a default block or COCO process simulator with the implementation of Matlab CAPE-OPEN v.2 unit operations. Although the expected best performance of the model, it has to be taken into account the fact that the inclusion of kinetic rates is computing expensive and also that might contain parameters that limit their application to different types of industrial realities.

Batch drying of sand in a draft-tube conical SB was satisfactory modelled by Olazar et al. [251]. A model based on mass balances using Matlab was able to predict the evolution of moisture content of gas and solids in the different regions of the SB dryer and, more interestingly, the end of drying period with high accuracy.

Following the unsatisfactory agreement between the correlations available in literature to describe the local heat transfer coefficients in SB reactors (mandatory for the correct design of drying processes), a new expression was obtained by Saldarriaga et al. [252] using a bed of sand and sawdust inside a conical SB reactor. The model was found valid for the definition of the most adequate position of heat transfer devices within the annulus of the reactor. This information could be used for optimising the best location of internal devices for heat recovery.

Given the particular fluid dynamic properties of the reactor, the related specific parameters should be included as main equations inside the proposed models. In this sense, Li et al. [253] outlined a 3D kinetic and computational fluid dynamic model for a pressurized spout-fluid bed and provided verification based on experimental data. Du et al. [211] proposed a hydrodynamic model based on an equivalent reactor network built in Aspen Plus<sup>®</sup> with gasification of polyethylene reactions are included through an external FORTRAN module. The good agreement of the model results with experimental data permitted to obtain valuable information regarding the influence of the gasification temperature and equivalence ratio on the gasification performance.

## 5. New Approaches: Neural Network Modelling

Artificial Neural Networks (ANN) have been extensively used in fields like pattern recognition, signal processing or robot control. In the recent years, this approach has been applied for the prediction of the behaviour of SB in a non-mechanistic way. Their main advantage resides in their capability of handling noisy and incomplete set of data and dealing with non-linear problems. The methodology is based on a first step of training where the model learns from examples and, once trained, is able to perform accurate predictions in very short periods of time.

Zhong and co-workers [254] developed a back-propagation neural network (BP-neural network) to predict the minimum spouting velocity by using 164 experimental data for training and validating the model. The model provided in some cases more accurate results respect to those obtained from traditional empirical correlations. In fact, these correlations are closely related to the experimental conditions used during their calculation, being valid only for a narrow window. This alternative shows promising results when the relation between geometric factors and operating parameters is complex and difficult to describe as it is the case with  $U_{ms}$ . Neural network models were also applied for the prediction of  $U_{ms}$  for a central jet SB and a circular slit SB achieving more accurate results than those obtained from correlations [255]. A Back Projection (BP)-algorithm was also used to determine the degree of coffee roasting based on colour images [256]. This way, the technical difficulties of commercial colorimeters for the detection of colour changes are successfully overcome.

Sometimes, a hybrid neural network is developed for process modelling. This approach combines a partial model based on the main principles of the process with a Multilayer Feed-Forward Neural network (MFFN) that is able to estimate the parameters that cannot be measured (or are difficult to be quantified from first principles). This is the case of the model developed by [257] and used to infer the moisture content of milk powder during its drying process. It was composed by one term which considered mass and energy balances and a second term which was estimated by an ANN. The whole description was included in an inferential controller whose parameters were tuned by trial and error. Another hybrid model was used to determine the moisture content of the powders produced during paste drying in a conical SB [7]. The effective drying kinetics were described by neural network and included in the overall mass and energy balances.

## 6. Concluding Remarks

The definition of accurate and efficient models to simulate processes occurring within an SB is still a major challenge for the development of the technology. Detailed modelling at different scales could have the key to achieve a reliable industrial scale application. Indeed, the definition of tools to facilitate multiphase reaction system scale-up, and system integration tools to consider micro, meso, and macro scales, were considered as fundamental needs within the roadmap for Reaction Engineering [258].

With this aim, numerical methods able to describe macroscopic behaviour of complex systems like SB need to be developed on the basis of microscopic models that can help understanding all the local involved phenomena. However, computational capabilities and the lack of physical realities to validate the models are characteristics that cannot be avoided.

In this framework, the performed multiscale analysis has shown that there is still a need of a deep understanding of phenomena at the single scales and also for their interrelations. In particular:

- *Molecular and particle scale*: the introduction of very specific parameters may provide more accurate modelling results but it will also limit the applicability of models to a short range of conditions. Moreover, kinetic schemes are very process specific, sometimes obtained with no physical sense, and their validity at large scale is still controversial. In addition, a further understanding and consensus of the role of drag forces and turbulence phenomena and the influence of shape and size distribution of particles is required for a successful advancement of the technology.
- *Reactor scale*: semi-empirical correlations for SB design are highly dependent on the geometry of the device and on the characteristics of the feedstock making difficult their applicability in a

wide range of situations. Also, the lack of devices in a larger scale does not permit the validation of the existing correlations at scales over lab applications where phenomena as heat transfer or chemical reactions are not likely to follow scale up strategies based on similitude of parameters.

- *Process scale*: at the moment, very few models have been proposed where kinetic or fluid dynamic properties are taken into account in a large scale framework. Also, the lack of experimental data at large scale difficults the validation of the models.

In conclusion, the definition of a robust multiscale model in which solid links between micro and macroscopic phenomena are defined with the correct balance between accuracy and computational costs might gear SB towards a reliable and successful implementation.

**Acknowledgments:** This work has been carried out in the framework of the project LIFE LIBERNITRATE funded by the EU under LIFE instrument (grant number LIFE 16 ENV/ES/000419).

**Author Contributions:** The work presented in this article is the result of a collaboration of all authors. Cristina Moliner and Filippo Marchelli analyzed the literature on the subject and wrote and edited the manuscript. Barbara Bosio and Elisabetta Arato critically reviewed the article and actively contributed to finalize the manuscript. All authors contributed to the discussion and conclusion of this research.

**Conflicts of Interest:** The authors declare no conflict of interest.

## Abbreviations and Symbols

$Ar$	Archimedes number
$D$	diameter of cylindrical column, m
$D_b$	upper diameter of static bed, m
$D_i$	diameter of fluid inlet, m
$D_0$	diameter of cone base, m
$D_s$	spout diameter, m
$d_p$	particle diameter, m
$e_s$	restitution coefficient
$G$	superficial mass flux of fluid, kg/m <sup>2</sup> s
$g$	acceleration of gravity, m/s <sup>2</sup>
$H$	bed depth, m
$H_0$	static bed depth, m
$H_f$	fountain height, measured from bed surface, m
$H_m$	maximum spoutable bed depth, m
$Re_{ms}$	Reynolds number based on $D_i$ , m/s
$U$	superficial velocity of spouting fluid based on $D$ , m/s
$U_i$	average fluid velocity at inlet, m/s
$U_{ms}$	superficial velocity at minimum spouting, m/s
$U_t$	free settling terminal velocity, m/s
$\Delta P_M$	maximum pressure drop across bed, Pa
$\Delta P_s$	spouting pressure drop across bed, Pa
$\varepsilon_0$	loose packed voidage
$\mu$	absolute viscosity, Pa·s
$\theta$	angle of cone, degrees or radian
$\phi$	sphericity
$\gamma$	inertial friction angle of particle, degree or radian
$\rho$	density of fluid, kg/m <sup>3</sup>
$\rho_b$	bulk density, kg/m <sup>3</sup>
$\rho_p$	density of particles, kg/m <sup>3</sup>

## References

1. Mathur, K.B.; Gishler, P.E. A technique for contacting gases with coarse solid particles. *AIChE J.* **1955**, *1*, 157–164. [[CrossRef](#)]

2. Gómez-Barea, A.; Leckner, B. Modeling of biomass gasification in fluidized bed. *Prog. Energy Combust. Sci.* **2010**, *36*, 444–509. [[CrossRef](#)]
3. Epstein, N.; Grace, J.R. *Spouted and Spout-Fluid Beds*; Epstein, N., Grace, J.R., Eds.; Cambridge University Press: Cambridge, UK, 2010; ISBN 9780511777936.
4. Brunello, G.; Peck, R.E.; Nina, G. Della The drying of barley malt in the spouted bed dryer. *Can. J. Chem. Eng.* **1974**, *52*, 201–205. [[CrossRef](#)]
5. Sodha, M.S.; Singh, N.P.; Chandra, R. Drying of paddy in a bed dryer. *Dry. Technol.* **1988**, *6*, 251–254. [[CrossRef](#)]
6. San José, M.J.; Álvarez, S.; López, L.B.; García, I. Drying of mixtures of agricultural wastes in a conical spouted bed contactor. *Chem. Eng. Trans.* **2011**, *24*, 673–678.
7. De Souza Nascimento, B.; Freire, F.B.; Freire, J.T. Neuronal and grey modelling of milk drying in spouted bed. *Can. J. Chem. Eng.* **2013**. [[CrossRef](#)]
8. Braga, M.B.; Wang, Z.; Grace, J.R.; Lim, C.J.; Rocha, S.C.S. Slot-Rectangular Spouted Bed: Hydrodynamic Stability and Effects of Operating Conditions on Drying Performance. *Dry. Technol. Int. J.* **2015**, *33*, 216–226. [[CrossRef](#)]
9. San Jose, M.J.; Alvarez, S.; Penas, F.J.; Garcia, I. Cycle time in draft tube conical spouted bed dryer for sludge from paper industry. *Chem. Eng. Sci.* **2013**, *100*, 413–420. [[CrossRef](#)]
10. De Alsina, O.L.S.; de Almeida, M.M.; da Silva, J.M.; Monteiro, L.F. *Drying of Fruits Pieces in Fixed and Spouted Bed*; Springer International Publishing: Basel, Switzerland, 2014; pp. 141–159.
11. Araújo, A.D.A.; Coelho, R.M.D.; Fontes, C.P.M.L.; Silva, A.R.A.; Da Costa, J.M.C.; Rodrigues, S. Production and spouted bed drying of acerola juice containing oligosaccharides. *Food Bioprod. Process.* **2015**, *94*, 565–571. [[CrossRef](#)]
12. Sousa, S.L.; De Morais, B.A.; Ribeiro, L.C.; Costa, J.M.C. Stability of cashew apple juice in powder dehydrated in spouted bed. *Rev. Bras. Eng. Agríc. Ambient.* **2016**, *20*, 678–682. [[CrossRef](#)]
13. Fakhre Dizaji, M.; HamidiSepehr, A.; Chegini, G.; Khazaei, J.; Mansuri, A. Influence of Hot Bed Spray Dryer Parameters on Physical Properties of Peppermint (*Mentha piperita* L.) Tea Powder. *Int. J. Food Eng.* **2015**, *11*, 115–125. [[CrossRef](#)]
14. Wang, S.; Yang, R.; Han, Y.; Gu, Z. Effect of three spouted drying methods on the process and quality characteristics of carrot cubes. In *Advanced Engineering and Technology II*; CRC Press: Boca Raton, FL, USA, 2015; pp. 301–307.
15. Chielle, D.P.; Bertuol, D.A.; Meili, L.; Tanabe, E.H.; Dotto, G.L. Spouted bed drying of papaya seeds for oil production. *LWT Food Sci. Technol.* **2016**, *65*, 852–860. [[CrossRef](#)]
16. Sahin, S.; Sumnu, G.; Tunaboyu, F. Usage of solar-assisted spouted bed drier in drying of pea. *Food Bioprod. Process.* **2013**, *91*, 271–278. [[CrossRef](#)]
17. Chen, F.; Zhang, M.; Mujumdar, A.S.; Jiang, H.; Wang, L. Production of Crispy Granules of Fish: A Comparative Study of Alternate Drying Techniques. *Dry. Technol.* **2014**, *32*, 1512–1521. [[CrossRef](#)]
18. Jindarat, W.; Sungsoontorn, S.; Rattanadecho, P. Analysis of Energy Consumption in a Combined Microwave-hot Air Spouted Bed Drying of Biomaterial: Coffee Beans. *Exp. Heat Transf.* **2014**, *28*, 107–124. [[CrossRef](#)]
19. Lu, Y.; Zhang, M.; Liu, H.; Mujumdar, A.S.; Sun, J.; Zheng, D. Optimization of Potato Cube Drying in a Microwave-Assisted Pulsed Spouted Bed. *Dry. Technol.* **2014**, *32*, 960–968. [[CrossRef](#)]
20. Mothibe, K.J.; Wang, C.-Y.; Mujumdar, A.S.; Zhang, M. Microwave-Assisted Pulse-Spouted Vacuum Drying of Apple Cubes. *Dry. Technol.* **2014**, *32*, 1762–1768. [[CrossRef](#)]
21. Qi, L.-L.; Zhang, M.; Mujumdar, A.S.; Meng, X.-Y.; Chen, H.-Z. Comparison of Drying Characteristics and Quality of Shiitake Mushrooms (*Lentinus edodes*) Using Different Drying Methods. *Dry. Technol.* **2014**, *32*, 1751–1761. [[CrossRef](#)]
22. Cao, X.; Zhang, M.; Fang, Z.; Mujumdar, A.S.; Jiang, H.; Qian, H.; Ai, H. Drying kinetics and product quality of green soybean under different microwave drying methods. *Dry. Technol. Int. J.* **2017**, *35*, 240–248. [[CrossRef](#)]
23. Conceição Filho, R.S.; Barrozo, M.A.S.; Limaverde, J.R.; Ataíde, C.H. The use of a spouted bed in the fertilizer coating of soybean seeds. *Dry. Technol.* **1998**, *16*, 2049–2064. [[CrossRef](#)]

24. Mollick, P.K.; Venugopalan, R.; Roy, M.; Rao, P.T.; Sathiyamoorthy, D.; Sengupta, P.; Sharma, G.; Basak, C.B.; Chakravartty, J.K. Deposition of diversely textured buffer pyrolytic carbon layer in TRISO coated particle by controlled manipulation of spouted bed hydrodynamics. *Chem. Eng. Sci.* **2015**, *128*, 44–53. [[CrossRef](#)]
25. Şentürk Lüle, S.; Colak, U.; Koksall, M.; Kulah, G. CFD Simulations of Hydrodynamics of Conical Spouted Bed Nuclear Fuel Coaters. *Chem. Vap. Depos.* **2015**, *21*, 122–132. [[CrossRef](#)]
26. Mai, X.; Zhang, F.; Lin, J.; Zhu, Z. Hydrodynamics of spouted bed in TRISO particle buffer layer coating process. *Nucl. Tech.* **2015**, *38*. [[CrossRef](#)]
27. Chen, W.Y.; Kuo, H.P. Surface coating of group B iron powders in a spouted bed. *Procedia Eng.* **2015**, *102*, 1144–1149. [[CrossRef](#)]
28. Plawsky, J.L.; Littman, H. *Design and Simulation of a Spout Fluid Bed Coating System*; Rensselaer Polytechnic Institute: Troy, NY, USA, 2006; Volume 7.
29. Da Rosa, G.S.; dos Santos Rocha, S.C. Use of vinasse to produce slow-release coated urea in spouted bed. *Can. J. Chem. Eng.* **2013**, *91*, 589–597. [[CrossRef](#)]
30. Ua-amnueychai, W.; Kodama, S.; Tanthapanichakoon, W.; Sekiguchi, H. Preparation of zinc coated PMMA using solid precursor by gliding arc discharge. *Chem. Eng. J.* **2015**, *278*, 301–308. [[CrossRef](#)]
31. Bilbao, J.; Olázar, M.; Romero, A.; Arandes, J.M. Design and operation of a jet spouted bed reactor with continuous catalyst feed in the benzyl alcohol polymerization. *Ind. Eng. Chem. Res.* **1987**, *26*, 1297–1304. [[CrossRef](#)]
32. Kechagiopoulos, P.N.; Voutetakis, S.S.; Vasalos, I.A. Sustainable hydrogen production via reforming of ethylene glycol using a novel spouted bed reactor. *Catal. Today* **2007**, *127*, 246–255. [[CrossRef](#)]
33. Wolff, M.F.H.; Salikov, V.; Antonyuk, S.; Heinrich, S.; Schneider, G.A. Novel, highly-filled ceramic-polymer composites synthesized by a spouted bed spray granulation process. *Compos. Sci. Technol.* **2014**, *90*, 154–159. [[CrossRef](#)]
34. Eichner, E.; Salikov, V.; Bassen, P.; Heinrich, S.; Schneider, G.A. Using dilute spouting for fabrication of highly filled metal-polymer composite materials. *Powder Technol.* **2016**. [[CrossRef](#)]
35. Handge, U.A.; Wolff, M.F.H.; Abetz, V.; Heinrich, S. Viscoelastic and dielectric properties of composites of poly(vinyl butyral) and alumina particles with a high filling degree. *Polymer* **2016**, *82*, 337–348. [[CrossRef](#)]
36. Xu, X.Y.; Lin, H.; Chen, X.; Zhao, B. Study on the Treatment of Nickel-Containing Wastewater by Spouted Bed Particulate Electro-Deposition. *Adv. Mater. Res.* **2013**, *864–867*, 1462–1465. [[CrossRef](#)]
37. El-Naas, M.H.; Alhaja, M.A.; Al-Zuhair, S. Evaluation of a three-step process for the treatment of petroleum refinery wastewater. *J. Environ. Chem. Eng.* **2014**, *2*, 56–62. [[CrossRef](#)]
38. Baghban, E.; Mehrabani-Zeinabad, A.; Moheb, A. The effects of operational parameters on the electrochemical removal of cadmium ion from dilute aqueous solutions. *Hydrometallurgy* **2014**, *149*, 97–105. [[CrossRef](#)]
39. Liu, D.; Roberts, E.P.L.; Martin, A.D.; Holmes, S.M.; Brown, N.W.; Campen, A.K.; de las Heras, N. Electrochemical regeneration of a graphite adsorbent loaded with Acid Violet 17 in a spouted bed reactor. *Chem. Eng. J.* **2016**, *304*, 1–9. [[CrossRef](#)]
40. Darwish, A.S.; Zewail, T.M.; Yousef, N.S.; El-Tawail, Y.A. Investigation of the performance of a batch air spouting bed in conducting ion exchange reactions involving heavy metal removal. *J. Taiwan Inst. Chem. Eng.* **2015**, *47*, 171–176. [[CrossRef](#)]
41. Watkinson, A.P.; Lisboa, A.C.L. Gasification, pyrolysis, and combustion. In *Spouted and Spout-Fluid Beds*; Epstein, N., Grace, J.R., Eds.; Cambridge University Press: Cambridge, UK, 2010; pp. 250–268.
42. Amutio, M.; Lopez, G.; Artetxe, M.; Elordi, G.; Olazar, M.; Bilbao, J. Influence of temperature on biomass pyrolysis in a conical spouted bed reactor. *Resour. Conserv. Recycl.* **2012**, *59*, 23–31. [[CrossRef](#)]
43. Du, S.; Sun, Y.; Gamliel, D.P.; Valla, J.A.; Bollas, G.M. Catalytic pyrolysis of miscanthus giganteus in a spouted bed reactor. *Bioresour. Technol.* **2014**, *169*, 188–197. [[CrossRef](#)] [[PubMed](#)]
44. Amutio, M.; Lopez, G.; Alvarez, J.; Olazar, M.; Bilbao, J. Fast pyrolysis of eucalyptus waste in a conical spouted bed reactor. *Bioresour. Technol.* **2015**, *194*, 225–232. [[CrossRef](#)] [[PubMed](#)]
45. Arregi, A.; Barbarias, I.; Alvarez, J.; Erkiaga, A.; Artetxe, M.; Amutio, M.; Olazar, M. Hydrogen Production from Biomass Pyrolysis and In-line Catalytic Steam Reforming. *Chem. Eng. Trans.* **2015**, *43*, 547–552.
46. Arregi, A.; Amutio, M.; Lopez, G.; Artetxe, M.; Alvarez, J.; Bilbao, J.; Olazar, M. Hydrogen-rich gas production by continuous pyrolysis and in-line catalytic reforming of pine wood waste and HDPE mixtures. *Energy Convers. Manag.* **2017**, *136*, 192–201. [[CrossRef](#)]

47. Makibar, J.; Fernandez-Akarregi, A.R.; Amutio, M.; Lopez, G.; Olazar, M. Performance of a conical spouted bed pilot plant for bio-oil production by poplar flash pyrolysis. *Fuel Process. Technol.* **2015**, *137*, 283–289. [[CrossRef](#)]
48. Aguado, R.; Olazar, M.; Gaisan, B.; Prieto, R.; Bilbao, J. Kinetic Study of Polyolefins Pyrolysis in a Conical Spouted Bed Reactor. *Ind. Eng. Chem. Res.* **2002**, *41*, 4559–4566. [[CrossRef](#)]
49. Aguado, R.; Prieto, R.; José, M.J.S.; Alvarez, S.; Olazar, M.; Bilbao, J. Defluidization modelling of pyrolysis of plastics in a conical spouted bed reactor. *Chem. Eng. Process. Process Intensif.* **2005**, *44*, 231–235. [[CrossRef](#)]
50. Olazar, M.; Aguado, R.; San José, M.J.; Alvarez, S.; Bilbao, J. Minimum spouting velocity for the pyrolysis of scrap tyres with sand in conical spouted beds. *Powder Technol.* **2006**, *165*, 128–132. [[CrossRef](#)]
51. Lopez, G.; Amutio, M.; Elordi, G.; Artetxe, M.; Altzibar, H.; Olazar, M. A conical spouted bed reactor for the valorisation of waste tires. In Proceedings of the 13th International Conference on Fluidisation—New Paradigm in Fluidisation Engineering, Gyeong-ju, Korea, 16–21 May 2010; pp. 1–8.
52. Alvarez, J.; Lopez, G.; Amutio, M.; Bilbao, J.; Olazar, M. Preparation of adsorbents from sewage sludge pyrolytic char by carbon dioxide activation. *Process Saf. Environ. Prot.* **2016**, *103*, 76–86. [[CrossRef](#)]
53. Alvarez, J.; Amutio, M.; Lopez, G.; Barbarias, I.; Bilbao, J.; Olazar, M. Sewage sludge valorization by flash pyrolysis in a conical spouted bed reactor. *Chem. Eng. J.* **2015**, *273*, 173–183. [[CrossRef](#)]
54. Alvarez, J.; Amutio, M.; Lopez, G.; Bilbao, J.; Olazar, M. Fast co-pyrolysis of sewage sludge and lignocellulosic biomass in a conical spouted bed reactor. *Fuel* **2015**, *159*, 810–818. [[CrossRef](#)]
55. Alvarez, J.; Lopez, G.; Amutio, M.; Artetxe, M.; Barbarias, I.; Arregi, A.; Bilbao, J.; Olazar, M. Characterization of the bio-oil obtained by fast pyrolysis of sewage sludge in a conical spouted bed reactor. *Fuel Process. Technol.* **2016**, *149*, 169–175. [[CrossRef](#)]
56. Rasul, M.G. Spouted bed combustion of wood charcoal: Performance comparison of three different designs. *Fuel* **2001**, *80*, 2189–2191. [[CrossRef](#)]
57. Albina, D.O. Emissions from multiple-spouted and spout-fluid fluidized beds using rice husks as fuel. *Renew. Energy* **2006**, *31*, 2152–2163. [[CrossRef](#)]
58. San José, M.J.; Alvarez, S.; García, I.; Peñas, F.J. A novel conical combustor for thermal exploitation of vineyard pruning wastes. *Fuel* **2013**, *110*, 178–184. [[CrossRef](#)]
59. San José, M.J.; Alvarez, S.; Peñas, F.J.; García, I. Thermal exploitation of fruit tree pruning wastes in a novel conical spouted bed combustor. *Chem. Eng. J.* **2014**, *238*, 227–233. [[CrossRef](#)]
60. San José, M.J.; Alvarez, S.; García, I.; Peñas, F.J. Conical spouted bed combustor for clean valorization of sludge wastes from paper industry to generate energy. *Chem. Eng. Res. Des.* **2014**, *92*, 672–678. [[CrossRef](#)]
61. Konduri, R.K.; Altwicker, E.R.; Morgan, M.H. Design and scale-up of a spouted-bed combustor. *Chem. Eng. Sci.* **1999**, *54*, 185–204. [[CrossRef](#)]
62. Tsuji, T.; Uemaki, O. Coal gasification in a jet-spouted bed. *Can. J. Chem. Eng.* **1994**, *72*, 504–510. [[CrossRef](#)]
63. Uemaki, O.; Tsuji, T. Gasification of a Sub-Bituminous Coal in a Two-Stage Jet Spouted Bed Reactor. In *Fluidization*; Engineering Foundation: New York, NY, USA, 1986; pp. 497–504.
64. Bernocco, D.; Bosio, B.; Arato, E. Feasibility study of a spouted bed gasification plant. *Chem. Eng. Res. Des.* **2013**, *91*, 843–855. [[CrossRef](#)]
65. Erkiaga, A.; Lopez, G.; Amutio, M.; Bilbao, J.; Olazar, M. Steam gasification of biomass in a conical spouted bed reactor with olivine and  $\gamma$ -alumina as primary catalysts. *Fuel Process. Technol.* **2013**, *116*, 292–299. [[CrossRef](#)]
66. Erkiaga, A.; Lopez, G.; Amutio, M.; Bilbao, J.; Olazar, M. Influence of operating conditions on the steam gasification of biomass in a conical spouted bed reactor. *Chem. Eng. J.* **2014**, *237*, 259–267. [[CrossRef](#)]
67. Bove, D.; Moliner, C.; Curti, M.; Rovero, G.; Baratieri, M.; Bosio, B.; Arato, E.; Garbarino, G.; Marchelli, F. Experimental studies on the gasification of the residues from prune of apple trees with a spouted bed reactor. In Proceedings of the European Biomass Conference and Exhibition, Amsterdam, The Netherlands, 6–9 June 2016; Volume 2016, pp. 858–862.
68. Adegoroye, A.; Paterson, N.; Li, X.; Morgan, T.; Herod, A.A.; Dugwell, D.R.; Kandiyoti, R. The characterisation of tars produced during the gasification of sewage sludge in a spouted bed reactor. *Fuel* **2004**, *83*, 1949–1960. [[CrossRef](#)]
69. Yasin, S.; Curti, M.; Rovero, G.; Behary, N.; Perwuelz, A.; Giraud, S.; Migliavacca, G.; Chen, G.; Guan, J. An Alternative for the End-of-life Phase of Flame Retardant Textile Products: Degradation of Flame Retardant and Preliminary Settings of Energy Valorization by Gasification. *BioResources* **2017**, *12*, 5196–5211. [[CrossRef](#)]

70. Sangtongam, K.; Gmurczyk, J.; Gupta, A.K. Parameters Influencing Clean Syngas Production from Biomass, Solid Wastes, and Coal during Steam Gasification. In Proceedings of the International Symposium on EcoTopia Science, Nagoya, Japan, 23–25 November 2007; pp. 617–622.
71. Beltramo, C.; Rovero, G.; Cavaglia, G. Hydrodynamic and thermal experimentation on square-based spouted beds for polymer upgrading and unit scale-up. *Can. J. Chem. Eng.* **2009**, *87*, 394–402. [[CrossRef](#)]
72. Makibar, J.; Fernandez-Akarregi, A.R.; Díaz, L.; Lopez, G.; Olazar, M. Pilot scale conical spouted bed pyrolysis reactor: Draft tube selection and hydrodynamic performance. *Powder Technol.* **2012**, *219*, 49–58. [[CrossRef](#)]
73. Paterson, N.; Reed, G.P.; Dugwell, D.R.; Kandiyoti, R. Gasification Tests With Sewage Sludge and Coal/Sewage Sludge Mixtures in a Pilot Scale, Air Blown, Spouted Bed Gasifier. In *Turbo Expo 2002*; ASME: Singapore, 2002; Volume 1, pp. 197–202.
74. Madhiyanon, T.; Soponronnarit, S.; Tia, W. Industrial-scale prototype of continuous spouted bed paddy dryer. *Dry. Technol.* **2001**, *19*, 207–216. [[CrossRef](#)]
75. Van der Hoef, M.A.; Ye, M.; van Sint Annaland, M.; Andrews, A.T.; Sundaresan, S.; Kuipers, J.A.M. Multiscale modeling of gas-fluidized beds. *Adv. Chem. Eng.* **2006**, *31*, 65–149.
76. Kechagiopoulos, P.N.; Voutetakis, S.S.; Lemonidou, A.A. Cold flow experimental study and computer simulations of a compact spouted bed reactor. *Chem. Eng. Process. Process Intensif.* **2014**, *82*, 137–149. [[CrossRef](#)]
77. Spreutels, L.; Haut, B.; Chaouki, J.; Bertrand, F.; Legros, R. Conical spouted bed drying of Baker's yeast: Experimentation and multi-modeling. *Food Res. Int.* **2014**, *62*, 137–150. [[CrossRef](#)]
78. Moliner, C.; Aguilar, K.; Bosio, B.; Arato, E.; Ribes, A. Thermo-oxidative characterisation of the residues from persimmon harvest for its use in energy recovery processes. *Fuel Process. Technol.* **2016**, *152*, 421–429. [[CrossRef](#)]
79. Moliner, C.; Bosio, B.; Arato, E.; Ribes, A. Thermal and thermo-oxidative characterisation of rice straw for its use in energy valorisation processes. *Fuel* **2016**, *180*, 71–79. [[CrossRef](#)]
80. Artetxe, M.; Lopez, G.; Amutio, M.; Barbarias, I.; Arregi, A.; Aguado, R.; Bilbao, J.; Olazar, M. Styrene recovery from polystyrene by flash pyrolysis in a conical spouted bed reactor. *Waste Manag.* **2015**, *45*, 126–133. [[CrossRef](#)] [[PubMed](#)]
81. Atutxa, A.; Aguado, R.; Gayubo, A.G.; Olazar, M.; Bilbao, J. Kinetic Description of the Catalytic Pyrolysis of Biomass in a Conical Spouted Bed Reactor. *Energy Fuels* **2005**, *19*, 765–774. [[CrossRef](#)]
82. Lopez, G.; Alvarez, J.; Amutio, M.; Arregi, A.; Bilbao, J.; Olazar, M. Assessment of steam gasification kinetics of the char from lignocellulosic biomass in a conical spouted bed reactor. *Energy* **2016**, *107*, 493–501. [[CrossRef](#)]
83. Niksiar, A.; Faramarzi, A.H.; Sohrabi, M. Kinetic study of polyethylene terephthalate (PET) pyrolysis in a spouted bed reactor. *AIChE J.* **2015**, *61*, 1900–1911. [[CrossRef](#)]
84. Olazar, M.; Lopez, G.; Arabiourrutia, M.; Elordi, G.; Aguado, R.; Bilbao, J. Kinetic modelling of tyre pyrolysis in a conical spouted bed reactor. *J. Anal. Appl. Pyrolysis* **2008**, *81*, 127–132. [[CrossRef](#)]
85. Amutio, M.; Lopez, G.; Aguado, R.; Artetxe, M.; Bilbao, J.; Olazar, M. Kinetic study of lignocellulosic biomass oxidative pyrolysis. *Fuel* **2012**, *95*, 305–311. [[CrossRef](#)]
86. Artetxe, M.; Lopez, G.; Amutio, M.; Bilbao, J.; Olazar, M. Kinetic modelling of the cracking of HDPE pyrolysis volatiles on a HZSM-5 zeolite based catalyst. *Chem. Eng. Sci.* **2014**, *116*, 635–644. [[CrossRef](#)]
87. Cundall, P.A.; Strack, O.D.L. A discrete numerical model for granular assemblies. *Géotechnique* **1979**, *29*, 47–65. [[CrossRef](#)]
88. Liu, D.; Bu, C.; Chen, X. Development and test of CFD–DEM model for complex geometry: A coupling algorithm for Fluent and DEM. *Comput. Chem. Eng.* **2013**, *58*, 260–268. [[CrossRef](#)]
89. Stroh, A.; Alobaid, F.; Hasenzahl, M.T.; Hilz, J.; Ströhle, J.; Epple, B. Comparison of three different CFD methods for dense fluidized beds and validation by a cold flow experiment. *Particuology* **2016**, *29*, 34–47. [[CrossRef](#)]
90. Alobaid, F. An offset-method for Euler-Lagrange approach. *Chem. Eng. Sci.* **2015**, *138*, 173–193. [[CrossRef](#)]
91. Golshan, S.; Esgandari, B.; Zarghami, R. CFD-DEM and TFM Simulations of Spouted Bed. *Chem. Eng. Trans.* **2017**, *57*, 1249–1254. [[CrossRef](#)]

92. Almohammed, N.; Alobaid, F.; Breuer, M.; Epple, B. A comparative study on the influence of the gas flow rate on the hydrodynamics of a gas–solid spouted fluidized bed using Euler–Euler and Euler–Lagrange/DEM models. *Powder Technol.* **2014**, *264*, 343–364. [[CrossRef](#)]
93. Pan, H.; Chen, X.-Z.; Liang, X.-F.; Zhu, L.-T.; Luo, Z.-H. CFD simulations of gas–liquid–solid flow in fluidized bed reactors—A review. *Powder Technol.* **2016**, *299*, 235–258. [[CrossRef](#)]
94. Tsuji, T.; Yabumoto, K.; Tanaka, T. Spontaneous structures in three-dimensional bubbling gas-fluidized bed by parallel DEM–CFD coupling simulation. *Powder Technol.* **2008**, *184*, 132–140. [[CrossRef](#)]
95. Golshan, S.; Zarghami, R.; Mostoufi, N. Hydrodynamics of slot-rectangular spouted beds: Process intensification. *Chem. Eng. Res. Des.* **2017**, *121*, 315–328. [[CrossRef](#)]
96. Zhang, H.; Li, S. DEM simulation of wet granular-fluid flows in spouted beds: Numerical studies and experimental verifications. *Powder Technol.* **2017**, *318*, 337–349. [[CrossRef](#)]
97. Saidi, M.; Wang, Z.; Grace, J.R.; Lim, C.J. Numerical and experimental investigation of hydrodynamic characteristics of a slot-rectangular spouted bed. *Can. J. Chem. Eng.* **2016**, *94*, 332–339. [[CrossRef](#)]
98. Zhang, H.; Li, S. Study on Drag Force Coefficients in Modeling Granular Flows in a Slot-Rectangular Spouted Bed. In Proceedings of the 7th International Conference on Discrete Element Methods, Dalian, China, 1–4 August 2016; pp. 697–707.
99. Qiu, K.; Hu, C.; Yang, S.; Luo, K.; Zhang, K.; Fan, J. Computational evaluation of depth effect on the hydrodynamics of slot-rectangular spouted bed. *Powder Technol.* **2016**, *287*, 51–60. [[CrossRef](#)]
100. Wen, Y.; Liu, M.; Liu, B.; Shao, Y. Comparative Study on the Characterization Method of Particle Mixing Index Using DEM Method. *Procedia Eng.* **2015**, *102*, 1630–1642. [[CrossRef](#)]
101. Liu, M.; Wen, Y.; Liu, R.; Liu, B.; Shao, Y. Investigation of fluidization behavior of high density particle in spouted bed using CFD-DEM coupling method. *Powder Technol.* **2015**, *280*, 72–82. [[CrossRef](#)]
102. Ren, B.; Zhong, W.; Jiang, X.; Jin, B.; Yuan, Z. Numerical simulation of spouting of cylindroid particles in a spouted bed. *Can. J. Chem. Eng.* **2014**, *92*, 928–934. [[CrossRef](#)]
103. Yang, S.; Luo, K.; Fang, M.; Fan, J. Discrete element simulation of the hydrodynamics in a 3D spouted bed: Influence of tube configuration. *Powder Technol.* **2013**, *243*, 85–95. [[CrossRef](#)]
104. Luo, K.; Yang, S.; Zhang, K.; Fang, M.; Fan, J. Particle dispersion and circulation patterns in a 3D spouted bed with or without draft tube. *Ind. Eng. Chem. Res.* **2013**, *52*, 9620–9631. [[CrossRef](#)]
105. Yang, S.; Luo, K.; Fang, M.; Zhang, K.; Fan, J. Three-Dimensional Modeling of Gas–Solid Motion in a Slot-Rectangular Spouted Bed with the Parallel Framework of the Computational Fluid Dynamics–Discrete Element Method Coupling Approach. *Ind. Eng. Chem. Res.* **2013**, *52*, 13222–13231. [[CrossRef](#)]
106. Marchelli, F.; Bove, D.; Moliner, C.; Bosio, B.; Arato, E. Discrete element method for the prediction of the onset velocity in a spouted bed. *Powder Technol.* **2017**, *321*, 119–131. [[CrossRef](#)]
107. Ren, B.; Zhong, W.; Chen, Y.; Chen, X.; Jin, B.; Yuan, Z.; Lu, Y. CFD-DEM simulation of spouting of corn-shaped particles. *Particuology* **2012**, *10*, 562–572. [[CrossRef](#)]
108. Ren, B.; Zhong, W.; Jin, B.; Shao, Y.; Yuan, Z. Numerical simulation on the mixing behavior of corn-shaped particles in a spouted bed. *Powder Technol.* **2013**, *234*, 58–66. [[CrossRef](#)]
109. Xie, J.; Zhong, W.; Jin, B. LES-Lagrangian modelling on gasification of combustible solid waste in a spouted bed. *Can. J. Chem. Eng.* **2014**, *92*, 1325–1333. [[CrossRef](#)]
110. Yang, S.; Luo, K.; Fang, M.; Fan, J. CFD-DEM simulation of the spout-annulus interaction in a 3D spouted bed with a conical base. *Can. J. Chem. Eng.* **2014**, *92*, 1130–1138. [[CrossRef](#)]
111. Zhou, L.; Zhang, L.; Bai, L.; Shi, W.; Li, W.; Wang, C.; Agarwal, R. Experimental study and transient CFD/DEM simulation in a fluidized bed based on different drag models. *RSC Adv.* **2017**, *7*, 12764–12774. [[CrossRef](#)]
112. Li, L.; Li, B.; Liu, Z. Modeling of spout-fluidized beds and investigation of drag closures using OpenFOAM. *Powder Technol.* **2017**, *305*, 364–376. [[CrossRef](#)]
113. Yang, S.; Sun, Y.; Zhang, L.; Zhao, Y.; Chew, J.W. Numerical investigation on the effect of draft plates on spouting stability and gas–solid characteristics in a spout-fluid bed. *Chem. Eng. Sci.* **2016**, *148*, 108–125. [[CrossRef](#)]
114. Banerjee, S.; Agarwal, R.K. Characterization of Scaling Laws in Computational Fluid Dynamics Simulations of Spouted Fluidized Beds for Chemical Looping Combustion. *Energy Fuels* **2016**, *30*, 8638–8647. [[CrossRef](#)]
115. Yang, S.; Sun, Y.; Wang, J.; Cahyadi, A.; Chew, J.W. Influence of operating parameters and flow regime on solid dispersion behavior in a gas-solid spout-fluid bed. *Chem. Eng. Sci.* **2016**, *142*, 112–125. [[CrossRef](#)]

116. Xu, H.; Zhong, W.; Yuan, Z.; Yu, A. CFD-DEM study on cohesive particles in a spouted bed. *Powder Technol.* **2016**. [[CrossRef](#)]
117. Sun, L.; Xu, W.; Lu, H.; Liu, G.; Zhang, Q.; Tang, Q.; Zhang, T. Simulated configurational temperature of particles and a model of constitutive relations of rapid-intermediate-dense granular flow based on generalized granular temperature. *Int. J. Multiph. Flow* **2015**, *77*, 1–18. [[CrossRef](#)]
118. Karimi, H.; Dehkordi, A.M. Prediction of equilibrium mixing state in binary particle spouted beds: Effects of solids density and diameter differences, gas velocity, and bed aspect ratio. *Adv. Powder Technol.* **2015**, *26*, 1371–1382. [[CrossRef](#)]
119. Wang, C.; Zhong, Z.; Wang, X.; Alting, S.A. Numerical simulation of gas-solid heat transfer behaviour in rectangular spouted bed. *Can. J. Chem. Eng.* **2015**, *93*, 2077–2083. [[CrossRef](#)]
120. Saidi, M.; Basirat Tabrizi, H.; Grace, J.R.; Lim, C.J. Hydrodynamic investigation of gas-solid flow in rectangular spout-fluid bed using CFD-DEM modeling. *Powder Technol.* **2015**, *284*, 355–364. [[CrossRef](#)]
121. Sutkar, V.S.; Deen, N.G.; Salikov, V.; Antonyuk, S.; Heinrich, S.; Kuipers, J.A.M. Experimental and numerical investigations of a pseudo-2D spout fluidized bed with draft plates. *Powder Technol.* **2015**, *270*, 537–547. [[CrossRef](#)]
122. Alobaid, F. A particle-grid method for Euler-Lagrange approach. *Powder Technol.* **2015**, *286*, 342–360. [[CrossRef](#)]
123. Wang, C.; Zhong, Z.; Wang, X.; Alting, S.A. Simulation of gas-solid flow in rectangular spouted bed by coupling CFD-DEM and LES. *Can. J. Chem. Eng.* **2014**, *92*, 1488–1494. [[CrossRef](#)]
124. Deb, S.; Tafti, D. Investigation of flat bottomed spouted bed with multiple jets using DEM-CFD framework. *Powder Technol.* **2014**, *254*, 387–402. [[CrossRef](#)]
125. Fan, J.; Xiao, G. Numerical Simulation of the Gas-Solid Flow by DEM-CFD Approach with Application to a Spouted Bed. *Sens. Transducers* **2014**, *164*, 218–226.
126. Alobaid, F.; Epple, B. Improvement, validation and application of CFD/DEM model to dense gas-solid flow in a fluidized bed. *Particuology* **2013**, *11*, 514–526. [[CrossRef](#)]
127. Sutkar, V.S.; Deen, N.G.; Mohan, B.; Salikov, V.; Antonyuk, S.; Heinrich, S.; Kuipers, J.A.M. Numerical investigations of a pseudo-2D spout fluidized bed with draft plates using a scaled discrete particle model. *Chem. Eng. Sci.* **2013**, *104*, 790–807. [[CrossRef](#)]
128. Ebrahimi, M.; Siegmann, E.; Prieling, D.; Glasser, B.J.; Khinast, J.G. An investigation of the hydrodynamic similarity of single-spout fluidized beds using CFD-DEM simulations. *Adv. Powder Technol.* **2017**, *28*, 2465–2481. [[CrossRef](#)]
129. Pietsch, S.; Heinrich, S.; Karpinski, K.; Müller, M.; Schönherr, M.; Kleine Jäger, F. CFD-DEM modeling of a three-dimensional prismatic spouted bed. *Powder Technol.* **2016**. [[CrossRef](#)]
130. Wang, Z.; Saidi, M.; Lim, C.J.; Grace, J.R.; Basirat Tabrizi, H.; Chen, Z.; Li, Y. Comparison of DEM simulation and experiments in a dual-column slot-rectangular spouted bed with a suspended partition. *Chem. Eng. J.* **2016**, *290*, 63–73. [[CrossRef](#)]
131. Zhang, L.; Wang, Z.; Wang, Q.; Qin, H.; Xu, X. Simulation of oil shale semi-coke particle cold transportation in a spouted bed using CPFD method. *Powder Technol.* **2016**, *301*, 360–368. [[CrossRef](#)]
132. Banerjee, S.; Agarwal, R. Transient reacting flow simulation of spouted fluidized bed for coal-direct chemical looping combustion with different Fe-based oxygen carriers. *Appl. Energy* **2015**, *160*, 552–560. [[CrossRef](#)]
133. Salikov, V.; Antonyuk, S.; Heinrich, S.; Sutkar, V.S.; Deen, N.G.; Kuipers, J.A.M. Characterization and CFD-DEM modelling of a prismatic spouted bed. *Powder Technol.* **2015**, *270*, 622–636. [[CrossRef](#)]
134. Banerjee, S.; Agarwal, R.K. Transient Reacting Flow Simulation of Spouted Fluidized Bed for Coal-Direct Chemical Looping Combustion. *J. Therm. Sci. Eng. Appl.* **2015**, *7*, 21016. [[CrossRef](#)]
135. Yang, S.; Luo, K.; Zhang, K.; Qiu, K.; Fan, J. Numerical study of a lab-scale double slot-rectangular spouted bed with the parallel CFD-DEM coupling approach. *Powder Technol.* **2015**, *272*, 85–99. [[CrossRef](#)]
136. Zhang, Z.; Zhou, L.; Agarwal, R. Transient Simulations of Spouted Fluidized Bed for Coal-Direct Chemical Looping Combustion. *Energy Fuels* **2014**, *28*, 1548–1560. [[CrossRef](#)]
137. Yang, S.; Luo, K.; Fang, M.; Zhang, K.; Fan, J. Parallel CFD-DEM modeling of the hydrodynamics in a lab-scale double slot-rectangular spouted bed with a partition plate. *Chem. Eng. J.* **2014**, *236*, 158–170. [[CrossRef](#)]
138. Fries, L.; Antonyuk, S.; Heinrich, S.; Dopfer, D.; Palzer, S. Collision dynamics in fluidised bed granulators: A DEM-CFD study. *Chem. Eng. Sci.* **2013**, *86*, 108–123. [[CrossRef](#)]

139. Bao, X.; Du, W.; Xu, J. Computational fluid dynamic modeling of spouted beds. In *Spouted and Spout-Fluid Beds*; Epstein, N., Grace, J.R., Eds.; Cambridge University Press: Cambridge, UK, 2010; pp. 57–81.
140. Bao, X.; Du, W.; Xu, J. An overview on the recent advances in computational fluid dynamics simulation of spouted beds. *Can. J. Chem. Eng.* **2013**, *91*, 1822–1836. [[CrossRef](#)]
141. Rong, L.W.; Zhan, J.M. Improved DEM-CFD model and validation: A conical-base spouted bed simulation study. *J. Hydrodyn.* **2010**, *22*, 351–359. [[CrossRef](#)]
142. Zhu, R.R.; Zhu, W.B.; Xing, L.C.; Sun, Q.Q. DEM simulation on particle mixing in dry and wet particles spouted bed. *Powder Technol.* **2011**, *210*, 73–81. [[CrossRef](#)]
143. Neto, J.L.V.; Duarte, C.R.; Murata, V.V.; Barrozo, M.A.S. Effect of a draft tube on the fluid dynamics of a spouted bed: Experimental and CFD studies. *Dry. Technol.* **2008**, *26*, 299–307. [[CrossRef](#)]
144. Schäfer, J.; Dippel, S.; Wolf, D.E. Force Schemes in Simulations of Granular Materials. *J. Phys. I* **1996**, *6*, 5–20. [[CrossRef](#)]
145. Di Renzo, A.; Di Maio, F.P. Comparison of contact-force models for the simulation of collisions in DEM-based granular flow codes. *Chem. Eng. Sci.* **2004**, *59*, 525–541. [[CrossRef](#)]
146. Tsuji, Y.; Tanaka, T.; Ishida, T. Lagrangian numerical simulation of plug flow of cohesionless particles in a horizontal pipe. *Powder Technol.* **1992**, *71*, 239–250. [[CrossRef](#)]
147. Tsuji, Y.; Kawaguchi, T.; Tanaka, T. Discrete particle simulation of two-dimensional fluidized bed. *Powder Technol.* **1993**, *77*, 79–87. [[CrossRef](#)]
148. Kobayashi, T.; Tanaka, T.; Shimada, N.; Kawaguchi, T. DEM-CFD analysis of fluidization behavior of Geldart Group A particles using a dynamic adhesion force model. *Powder Technol.* **2013**, *248*, 143–152. [[CrossRef](#)]
149. Alizadeh, E.; Bertrand, F.; Chaouki, J. Comparison of DEM results and Lagrangian experimental data for the flow and mixing of granules in a rotating drum. *AIChE J.* **2014**, *60*, 60–75. [[CrossRef](#)]
150. Campbell, C.S.; Brennen, C.E. Computer simulation of granular shear flows. *J. Fluid Mech.* **1985**, *151*, 167. [[CrossRef](#)]
151. Snider, D.M. An Incompressible Three-Dimensional Multiphase Particle-in-Cell Model for Dense Particle Flows. *J. Comput. Phys.* **2001**, *170*, 523–549. [[CrossRef](#)]
152. Hoomans, B.P.B. *Granular Dynamics of Gas-Solid Two-Phase Flow*; Twente University: Enschede, The Netherlands, 2000.
153. Zhu, H.P.; Zhou, Z.Y.; Yang, R.Y.; Yu, A.B. Discrete particle simulation of particulate systems: A review of major applications and findings. *Chem. Eng. Sci.* **2008**, *63*, 5728–5770. [[CrossRef](#)]
154. Gidaspow, D.; Bezburuah, R.; Ding, J. Hydrodynamics of Circulating Fluidized Beds, Kinetic Theory Approach. In Proceedings of the 7th Engineering Foundation Conference on Fluidization, Gold Coast, Australia, 3–8 May 1992; pp. 75–82.
155. Chen, F.; Qiang, H.; Gao, W. Coupling of smoothed particle hydrodynamics and finite volume method for two-dimensional spouted beds. *Comput. Chem. Eng.* **2015**, *77*, 135–146. [[CrossRef](#)]
156. Koch, D.L.; Hill, R.G. Inertial Effects in Suspensions and Porous-Media Flows. *Annu. Rev. Fluid Mech.* **2001**, *33*, 619–647. [[CrossRef](#)]
157. Beetstra, R.; Van Der Hoef, M.A.; Kuipers, J.A.M. Drag force of intermediate reynolds number flow past mono- and bidisperse arrays of spheres. *AIChE J.* **2007**, *53*, 489–501. [[CrossRef](#)]
158. Syamlal, M.; O'Brien, T. Computer simulation of bubbles in a fluidized bed. *AIChE Symp. Ser.* **1989**, *85*, 22–31.
159. Wen, C.Y.; Yu, Y.H. Mechanics of Fluidization. *Chem. Eng. Prog. Symp. Ser.* **1966**, *162*, 100–111.
160. Hill, R.G.; Koch, D.L.; Ladd, A.J.C. Moderate-Reynolds-number flows in ordered and random arrays of spheres. *J. Fluid Mech.* **2001**, *448*. [[CrossRef](#)]
161. Dahl, S.R.; Hrenya, C.M. Size segregation in gas–solid fluidized beds with continuous size distributions. *Chem. Eng. Sci.* **2005**, *60*, 6658–6673. [[CrossRef](#)]
162. Di Felice, R. The voidage function for fluid-particle interaction systems. *Int. J. Multiph. Flow* **1994**, *20*, 153–159. [[CrossRef](#)]
163. Haider, A.; Levenspiel, O. Drag coefficient and terminal velocity of spherical and nonspherical particles. *Powder Technol.* **1989**, *58*, 63–70. [[CrossRef](#)]
164. Pepiot, P.; Desjardins, O. Numerical analysis of the dynamics of two- and three-dimensional fluidized bed reactors using an Euler–Lagrange approach. *Powder Technol.* **2012**, *220*, 104–121. [[CrossRef](#)]

165. Ren, B.; Zhong, W.; Jin, B.; Lu, Y.; Chen, X.; Xiao, R. Study on the Drag of a Cylinder-Shaped Particle in Steady Upward Gas Flow. *Ind. Eng. Chem. Res.* **2011**, *50*, 7593–7600. [[CrossRef](#)]
166. Van Der Hoef, M.A.; Beetstra, R.; Kuipers, J.A.M. Lattice-Boltzmann simulations of low-Reynolds-number flow past mono- and bidisperse arrays of spheres: Results for the permeability and drag force. *J. Fluid Mech.* **2005**, *528*, 233–254. [[CrossRef](#)]
167. Ren, B.; Shao, Y.; Zhong, W.; Jin, B.; Yuan, Z.; Lu, Y. Investigation of mixing behaviors in a spouted bed with different density particles using discrete element method. *Powder Technol.* **2012**, *222*, 85–94. [[CrossRef](#)]
168. Lu, L.; Konan, A.; Benyahia, S. Influence of grid resolution, parcel size and drag models on bubbling fluidized bed simulation. *Chem. Eng. J.* **2017**. [[CrossRef](#)]
169. Shi, Z.; Wang, W.; Li, J. A bubble-based EMMS model for gas–solid bubbling fluidization. *Chem. Eng. Sci.* **2011**, *66*, 5541–5555. [[CrossRef](#)]
170. Glicksman, L.R.; Hyre, M.; Woloshun, K. Simplified scaling relationships for fluidized beds. *Powder Technol.* **1993**, *77*, 177–199. [[CrossRef](#)]
171. Link, J.M.; Godlieb, W.; Tripp, P.; Deen, N.G.; Heinrich, S.; Kuipers, J.A.M.; Schönherr, M.; Peglow, M. Comparison of fibre optical measurements and discrete element simulations for the study of granulation in a spout fluidized bed. *Powder Technol.* **2009**, *189*, 202–217. [[CrossRef](#)]
172. Zhong, W.; Yu, A.; Liu, X.; Tong, Z.; Zhang, H. DEM/CFD-DEM Modelling of Non-spherical Particulate Systems: Theoretical Developments and Applications. *Powder Technol.* **2016**, *302*, 108–152. [[CrossRef](#)]
173. Berger, K.J.; Hrenya, C.M. Challenges of DEM: II. Wide particle size distributions. *Powder Technol.* **2014**, *264*, 627–633. [[CrossRef](#)]
174. Elghobashi, S. On predicting particle-laden turbulent flows. *Appl. Sci. Res.* **1994**, *52*, 309–329. [[CrossRef](#)]
175. Zhao, X.L.; Li, S.Q.; Liu, G.Q.; Yao, Q.; Marshall, J.S. DEM simulation of the particle dynamics in two-dimensional spouted beds. *Powder Technol.* **2008**, *184*, 205–213. [[CrossRef](#)]
176. Vreman, A.W. An eddy-viscosity subgrid-scale model for turbulent shear flow: Algebraic theory and applications. *Phys. Fluids* **2004**, *16*, 3670–3681. [[CrossRef](#)]
177. Saidi, M.; Tabrizi, H.B. Numerical Investigation of Particles in a Gas-Solid Spouted Fluidized Bed. In Proceedings of the Particle Technology Forum 2014—Core Programming Area at the 2014 AIChE Annual Meeting, Atlanta, GA, USA, 16–21 November 2014.
178. Gao, J.; Lan, X.; Fan, Y.; Chang, J.; Wang, G.; Lu, C.; Xu, C. Hydrodynamics of gas–solid fluidized bed of disparately sized binary particles. *Chem. Eng. Sci.* **2009**, *64*, 4302–4316. [[CrossRef](#)]
179. Moliner Estopiñán, C.E. Valorisation of Agricultural Residues. Ph.D. Thesis, Universitat Politècnica de València, Valencia, Spain, 2016.
180. Mikami, T.; Kamiya, H.; Horio, M. Numerical simulation of cohesive powder behavior in a fluidized bed. *Chem. Eng. Sci.* **1998**, *53*, 1927–1940. [[CrossRef](#)]
181. Zhong, W.; Yu, A.; Zhou, G.; Xie, J.; Zhang, H. CFD simulation of dense particulate reaction system: Approaches, recent advances and applications. *Chem. Eng. Sci.* **2016**, *140*, 16–43. [[CrossRef](#)]
182. Finnie, I. Erosion of surfaces by solid particles. *Wear* **1960**, *3*, 87–103. [[CrossRef](#)]
183. Fane, A.G.; Mitchell, R.A. Minimum spouting velocity of scaled-up beds. *Can. J. Chem. Eng.* **1984**, *62*, 437–439. [[CrossRef](#)]
184. Yang, L.; Lim, J.C.; Epstein, N. Aerodynamic aspects of spouted beds at temperatures up to 580 °C. *J. Serbian Chem. Soc.* **1996**, *61*, 253–266.
185. Olazar, M.; San José, M.J.; Aguayo, A.T.; Arandes, J.M.; Bilbao, J. Hydrodynamics of nearly flat base spouted beds. *Chem. Eng. J. Biochem. Eng. J.* **1994**, *55*, 27–37. [[CrossRef](#)]
186. Anabtawi, M.Z.; Uysal, B.Z.; Jumah, R.Y. Flow characteristics in a rectangular spout-fluid bed. *Powder Technol.* **1992**, *69*, 205–211. [[CrossRef](#)]
187. Saldarriaga, J.F.; Aguado, R.; Altzibar, H.; Atxutegi, A.; Bilbao, J.; Olazar, M. Minimum spouting velocity for conical spouted beds of vegetable waste biomasses. *J. Taiwan Inst. Chem. Eng.* **2016**, *60*, 509–519. [[CrossRef](#)]
188. Manurung, F. Studies in the Spouted Bed Technique with Particular Reference to Low Temperature Coal Carbonization. Ph.D. Thesis, University of New South Wales, Kensington, Australia, 1964.
189. Kmie, A. Hydrodynamics of Flows and Heat Transfer in Spouted Beds. *Chem. Eng. J.* **1980**, *19*, 189–200. [[CrossRef](#)]
190. Olazar, M.; San José, M.J.; Aguayo, A.T.; Arandes, J.M.; Bilbao, J. Pressure drop in conical spouted beds. *Chem. Eng. J.* **1993**, *51*, 53–60. [[CrossRef](#)]

191. Markowski, A.; Kaminski, W. Hydrodynamic characteristics of jet-spouted beds. *Can. J. Chem. Eng.* **1983**, *61*, 377–381. [[CrossRef](#)]
192. San José, M.J.; Olazar, M.; Alvarez, S.; Morales, A.; Bilbao, J. Spout and Fountain Geometry in Conical Spouted Beds Consisting of Solids of Varying Density. *Ind. Eng. Chem. Res.* **2006**, *44*, 193–200.
193. Olazar, M.; Lopez, G.; Altzibar, H.; Barona, A.; Bilbao, J. One-dimensional modelling of conical spouted beds. *Chem. Eng. Process. Process Intensif.* **2009**, *48*, 1264–1269. [[CrossRef](#)]
194. Niksiar, A.; Sohrabi, M. A novel hydrodynamic model for conical spouted beds based on streamtube modeling approach. *Powder Technol.* **2014**, *267*, 371–380. [[CrossRef](#)]
195. Bridgwater, G.S.; McNab, J. Spouted beds—Estimation of spouting pressure drop and the particle size for deepest bed. In Proceedings of the European Congress on Particle Technology, Nuremberg, Germany, 24–25 May 1977; p. 17.
196. Lefroy, G.A.; Davidson, J. The mechanics of spouted beds. *Trans. Inst. Chem. Eng.* **1969**, *47*, 120–128.
197. He, Y.-L.; Lim, C.J.; Grace, J.R. Scale-up studies of spouted beds. *Chem. Eng. Sci.* **1997**, *52*, 329–339. [[CrossRef](#)]
198. Glicksman, L.R. Scaling relationships for fluidized beds. *Chem. Eng. Sci.* **1984**, *39*, 1373–1379. [[CrossRef](#)]
199. Huilin, L.; Yurong, H.; Wentie, L.; Ding, J.; Gidaspow, D.; Bouillard, J. Computer simulations of gas-solid flow in spouted beds using kinetic-frictional stress model of granular flow. *Chem. Eng. Sci.* **2004**, *59*, 865–878. [[CrossRef](#)]
200. Ali, N.; Al-Juwaya, T.; Al-Dahhan, M. An advanced evaluation of spouted beds scale-up for coating TRISO nuclear fuel particles using Radioactive Particle Tracking (RPT). *Exp. Therm. Fluid Sci.* **2017**, *80*, 90–104. [[CrossRef](#)]
201. Aradhya, S.; Taofeeq, H.; Al-dahhan, M. Evaluation of the Dimensionless Groups Based Scale-Up of Gas-Solid Spouted Beds. *Int. J. Multiph. Flow* **2017**. [[CrossRef](#)]
202. Setarehshenas, N.; Hosseini, S.H.; Esfahany, M.N.; Ahmadi, G. Three-dimensional CFD study of conical spouted beds containing heavy particles: Design parameters. *Korean J. Chem. Eng.* **2017**, *34*, 1541–1553. [[CrossRef](#)]
203. Reza, M.O.; Laugwitz, A.; Nikrityuk, P. Cylindrical-conical spouted bed dynamics: Laminar and turbulent flow predictions. *Can. J. Chem. Eng.* **2016**. [[CrossRef](#)]
204. Du, W.; Zhang, J.; Bao, S.; Xu, J.; Zhang, L. Numerical investigation of particle mixing and segregation in spouted beds with binary mixtures of particles. *Powder Technol.* **2016**, *301*, 1159–1171. [[CrossRef](#)]
205. Setarehshenas, N.; Hosseini, S.H.H.; Esfahany, M.N.; Ahmadi, G. Impacts of solid-phase wall boundary condition on CFD simulation of conical spouted beds containing heavy zirconia particles. *J. Taiwan Inst. Chem. Eng.* **2016**, *64*, 146–156. [[CrossRef](#)]
206. Melo, J.L.Z.; Baelos, M.S.; Pereira, F.A.R.; Lira, T.S.; Gidaspow, D. CFD modeling of conical spouted beds for processing LDPE/Al composite. *Chem. Eng. Process. Process Intensif.* **2016**, *108*, 93–108. [[CrossRef](#)]
207. Jin, G.; Zhang, M.; Fang, Z.; Cui, Z.; Song, C. Numerical Investigation on Effect of Food Particle Mass on Spout Elevation of a Gas-Particle Spout Fluidized Bed in a Microwave-Vacuum Dryer. *Dry. Technol.* **2015**, *33*, 591–604. [[CrossRef](#)]
208. Santos, K.G.; Francisquetti, M.C.C.; Malagoni, R.A.; Barrozo, M.A.S. Fluid Dynamic Behavior in a Spouted Bed with Binary Mixtures Differing in Size. *Dry. Technol.* **2015**, 1–12. [[CrossRef](#)]
209. Bove, D.; Moliner, C.; Bosio, B.; Arato, E.; Curti, M.; Rovero, G. CFD Simulations of a Square-Based Spouted Bed Reactor and Validation with Experimental Tests Using Rice Straw as Feedstock. *Chem. Eng. Trans.* **2015**, *43*, 1363–1368. [[CrossRef](#)]
210. Wang, S.; Shao, B.; Liu, R.; Zhao, J.; Liu, Y.; Liu, Y.; Yang, S. Comparison of numerical simulations and experiments in conical gas-solid spouted bed. *Chin. J. Chem. Eng.* **2015**, *23*, 1579–1586. [[CrossRef](#)]
211. Du, Y.; Yang, Q.; Berrouk, A.S.; Yang, C.; Al Shoaibi, A.S. Equivalent Reactor Network Model for Simulating the Air Gasification of Polyethylene in a Conical Spouted Bed Gasifier. *Energy Fuels* **2014**, *28*, 6830–6840. [[CrossRef](#)]
212. Liu, M.; Liu, B.; Shao, Y.; Wang, J. Optimization design of the coating furnace by 3-d simulation of spouted bed dynamics in the coater. *Nucl. Eng. Des.* **2014**, *271*, 68–72. [[CrossRef](#)]
213. Chaiwang, P.; Gidaspow, D.; Chalermwong, B.; Piumsomboon, P. CFD design of a sorber for CO<sub>2</sub> capture with 75 and 375 micron particles. *Chem. Eng. Sci.* **2014**, *105*, 32–45. [[CrossRef](#)]
214. Jin, G.; Zhang, M.; Fang, Z.; Cui, Z.; Song, C. Numerical study on spout elevation of a gas-particle spout fluidized bed in microwave-vacuum dryer. *J. Food Eng.* **2014**, *143*, 8–16. [[CrossRef](#)]

215. Jiang, X.; Zhong, W.; Liu, X.; Jin, B. Study on gas-solid flow behaviors in a spouted bed at elevated pressure: Numerical simulation aspect. *Powder Technol.* **2014**, *264*, 22–30. [[CrossRef](#)]
216. Wang, S.; Zhao, L.; Wang, C.; Liu, Y.; Gao, J.; Liu, Y.; Cheng, Q. Numerical simulation of gas–solid flow with two fluid model in a spouted-fluid bed. *Particuology* **2014**, *14*, 109–116. [[CrossRef](#)]
217. Riera, J.; Zeppieri, S.; Derjani-Bayeh, S. Hydrodynamic study of a multiphase spouted column. *Fuel* **2014**, *138*, 183–192. [[CrossRef](#)]
218. Hosseini, S.H.; Ahmadi, G.; Olazar, M. CFD study of particle velocity profiles inside a draft tube in a cylindrical spouted bed with conical base. *J. Taiwan Inst. Chem. Eng.* **2014**, *45*, 2140–2149. [[CrossRef](#)]
219. Liu, P.; Hrenya, C.M. Challenges of DEM: I. Competing bottlenecks in parallelization of gas-solid flows. *Powder Technol.* **2014**, *264*, 620–626. [[CrossRef](#)]
220. Hosseini, S.H.; Fattahi, M.; Ahmadi, G. Hydrodynamics studies of a pseudo 2D rectangular spouted bed by CFD. *Powder Technol.* **2015**, *279*, 301–309. [[CrossRef](#)]
221. Tabatabaei, S.A.; Mahinpey, N.; Esmaili, E.; Lim, C.J. CFD simulation of flow regime maps in a slot-rectangular spouted bed. *Can. J. Chem. Eng.* **2013**, *91*. [[CrossRef](#)]
222. Du, W.; Xu, J.; Wei, W.; Bao, X. Computational fluid dynamics validation and comparison analysis of scale-up relationships of spouted beds. *Can. J. Chem. Eng.* **2013**, *91*. [[CrossRef](#)]
223. Bie, W.B.; Szrednicki, G.; Fletcher, D.F. Hydrodynamics modeling of corn drying in a triangular spouted bed dryer. *Acta Hort.* **2013**, 169–178. [[CrossRef](#)]
224. Liu, X.; Shao, Y.; Zhong, W.; Grace, J.R.; Epstein, N.; Jin, B. Prediction of minimum spouting velocity by CFD-TFM: Approach development. *Can. J. Chem. Eng.* **2013**, *91*, 1800–1808. [[CrossRef](#)]
225. Zhong, W.; Liu, X.; Grace, J.R.; Epstein, N.; Ren, B.; Jin, B. Prediction of minimum spouting velocity of spouted bed by CFD-TFM: Scale-up. *Can. J. Chem. Eng.* **2013**, *91*. [[CrossRef](#)]
226. Moradi, S.; Yeganeh, A.; Salimi, M. CFD-modeling of effects of draft tubes on operating condition in spouted beds. *Appl. Math. Model.* **2013**, *37*, 1851–1859. [[CrossRef](#)]
227. Hosseini, S.H.; Ahmadi, G.; Olazar, M. CFD simulation of cylindrical spouted beds by the kinetic theory of granular flow. *Powder Technol.* **2013**, *246*, 303–316. [[CrossRef](#)]
228. Fattahi, M.; Hosseini, S.H.; Ahmadi, G. CFD simulation of transient gas to particle heat transfer for fluidized and spouted regimes. *Appl. Therm. Eng.* **2016**, *105*, 385–396. [[CrossRef](#)]
229. Hosseini, S.H.; Fattahi, M.; Ahmadi, G. CFD Study of hydrodynamic and heat transfer in a 2D spouted bed: Assessment of radial distribution function. *J. Taiwan Inst. Chem. Eng.* **2016**, *58*, 107–116. [[CrossRef](#)]
230. Wang, X.; Jin, B.; Wang, Y.; Hu, C. Three-dimensional multi-phase simulation of the mixing and segregation of binary particle mixtures in a two-jet spout fluidized bed. *Particuology* **2015**, *22*, 185–193. [[CrossRef](#)]
231. Chen, D.; Liu, X.; Zhong, W.; Shao, Y.; Jin, B. Interactions of spout jets in a multiple-spouted bed. *Can. J. Chem. Eng.* **2014**, *92*, 1150–1159. [[CrossRef](#)]
232. Liu, X.; Zhong, W.; Yu, A.; Xu, B.; Lu, J. Mixing behaviors in an industrial-scale spout-fluid mixer by 3D CFD-TFM. *Powder Technol.* **2016**. [[CrossRef](#)]
233. Gidaspow, D. *Multiphase Flow and Fluidization: Continuum and Kinetic Theory Descriptions*; Academic Press: Cambridge, MA, USA, 1994; ISBN 9780080512266.
234. Béttega, R.; Corrêa, R.G.; Freire, J.T. Use of Fluid Dynamic Simulation to Improve the Design of Spouted Beds. In *Applied Computational Fluid Dynamics*; InTech: Rijeka, Croatia, 2012; pp. 321–344. ISBN 978-953-51-0271-7.
235. Béttega, R.; Corrêa, R.G.; Freire, J.T. Scale-up study of spouted beds using computational fluid dynamics. *Can. J. Chem. Eng.* **2009**, *87*, 193–203. [[CrossRef](#)]
236. Liu, X.; Zhong, W.; Shao, Y.; Ren, B.; Jin, B. Evaluation on the effect of conical geometry on flow behaviours in spouted beds. *Can. J. Chem. Eng.* **2014**, *92*, 768–774. [[CrossRef](#)]
237. Prieur Du Plessis, J. Analytical quantification of coefficients in the Ergun equation for fluid friction in a packed bed. *Transp. Porous Media* **1994**, *16*, 189–207. [[CrossRef](#)]
238. Esmaili, E.; Mahinpey, N. Adjustment of drag coefficient correlations in three dimensional CFD simulation of gas–solid bubbling fluidized bed. *Adv. Eng. Softw.* **2011**, *42*, 375–386. [[CrossRef](#)]
239. Launder, B.E.; Spalding, D.B. The numerical computation of turbulent flows. *Comput. Methods Appl. Mech. Eng.* **1974**, *3*, 269–289. [[CrossRef](#)]
240. Wilcox, D.C. Reassessment of the scale-determining equation for advanced turbulence models. *AIAA J.* **1988**, *26*, 1299–1310. [[CrossRef](#)]

241. Menter, F.R. Two-equation eddy-viscosity turbulence models for engineering applications. *AIAA J.* **1994**, *32*, 1598–1605. [[CrossRef](#)]
242. Gunn, D.J. Transfer of heat or mass to particles in fixed and fluidised beds. *Int. J. Heat Mass Transf.* **1978**, *21*, 467–476. [[CrossRef](#)]
243. Lun, C.K.K.; Savage, S.B. The effects of an impact velocity dependent coefficient of restitution on stresses developed by sheared granular materials. *Acta Mech.* **1986**, *63*, 15–44. [[CrossRef](#)]
244. Ma, D.; Ahmadi, G. An equation of state for dense rigid sphere gases. *J. Chem. Phys.* **1986**, *84*, 3449–3450. [[CrossRef](#)]
245. Iddir, H.; Arastoopour, H. Modeling of multitype particle flow using the kinetic theory approach. *AIChE J.* **2005**, *51*, 1620–1632. [[CrossRef](#)]
246. Chen, Z.; Lim, C.J.; Grace, J.R. Stability of slot-rectangular spouted beds with multiple slots. *Can. J. Chem. Eng.* **2013**, *91*. [[CrossRef](#)]
247. Moliner, C.; Bove, D.; Bosio, B.; Ribes, A.; Arato, E. Feasibility studies on the energy valorisation of agricultural residues using Aspen Plus<sup>®</sup>. In Proceedings of the 23rd European Biomass Conference and Exhibition, Vienna, Austria, 1–4 June 2015; Volume 2015, pp. 803–809.
248. Jarungthammachote, S.; Dutta, A. Equilibrium modeling of gasification: Gibbs free energy minimization approach and its application to spouted bed and spout-fluid bed gasifiers. *Energy Convers. Manag.* **2008**, *49*, 1345–1356. [[CrossRef](#)]
249. Moliner, C.; Bove, D.; Bosio, B.; Ribes Greus, A.; Arato, E. Simulation activities for the pseudo-equilibrium modelling of the gasification of agricultural residues. In Proceedings of the European Biomass Conference and Exhibition, Amsterdam, The Netherlands, 6–9 June 2016; Volume 2016, pp. 934–940.
250. Kersten, S.; Palz, W.; Spitzer, J.; Prins, W.; Van der Drift, A.; Maniatis, K.; Kwant, K.; Helm, P.; Grassi, A. Interpretation of biomass gasification by “quasi” equilibrium models. In Proceedings of the 12th European Conference on Biomass for Energy, Industry and Climate Protection, Amsterdam, The Netherlands, 17–21 June 2002.
251. Olazar, M.; Lopez, G.; Altzibar, H.; Bilbao, J. Modelling batch drying of sand in a draft-tube conical spouted bed. *Chem. Eng. Res. Des.* **2011**, *89*, 2054–2062. [[CrossRef](#)]
252. Saldarriaga, J.F.; Aguado, R.; Atxutegi, A.; Grace, J.; Bilbao, J.; Olazar, M. Correlation for Calculating Heat Transfer Coefficient in Conical Spouted Beds. *Ind. Eng. Chem. Res.* **2016**, *55*, 9524–9532. [[CrossRef](#)]
253. Li, Q.; Zhang, M.; Zhong, W.; Wang, X.; Xiao, R. Simulation of Coal Gasification in a Pressurized Spout-Fluid Bed Gasifier. *Can. J. Chem. Eng.* **2009**, *87*, 169–176. [[CrossRef](#)]
254. Zhong, W.; Chen, X.; Grace, J.R.; Epstein, N.; Jin, B. Intelligent prediction of minimum spouting velocity of spouted bed by back propagation neural network. *Powder Technol.* **2013**, *247*, 197–203. [[CrossRef](#)]
255. Salam, P.A.; Bhattacharya, S.C. A comparative hydrodynamic study of two types of spouted bed reactor designs. *Chem. Eng. Sci.* **2006**, *61*, 1946–1957. [[CrossRef](#)]
256. Virgen-Navarro, L.; Herrera-López, E.J.; Corona-González, R.I.; Arriola-Guevara, E.; Guatemala-Morales, G.M. Neuro-fuzzy model based on digital images for the monitoring of coffee bean color during roasting in a spouted bed. *Expert Syst. Appl.* **2016**, *54*, 162–169. [[CrossRef](#)]
257. Nakamura Alves Vieira, G.; Bentes Freire, F.; Freire, J.T. Control of the Moisture Content of Milk Powder Produced in a Spouted Bed Dryer Using a Grey-Box Inferential Controller. *Dry. Technol.* **2015**, *33*, 1920–1928. [[CrossRef](#)]
258. Klipstein, D.H.; Robinson, S. *Vision 2020: Reaction Engineering Roadmap*; American Institute of Chemical Engineers: New York, NY, USA, 2001.

